

AWARD NUMBER: W81XWH-13-1-0303

TITLE:

Characterizing and Targeting Bone Marrow-Derived
Inflammatory Cells in Driving the Malignancy and Progression
of Childhood Astrocytic Brain Tumors

PRINCIPAL INVESTIGATOR: Yujie Huang Ph.D.

CONTRACTING ORGANIZATION:

Cornell University, Weill Cornell Medical College
New York, NY 10065-4805

REPORT DATE: September 2015

TYPE OF REPORT: Annual Report

PREPARED FOR: U.S. Army Medical Research and Materiel Command
Fort Detrick, Maryland 21702-5012

DISTRIBUTION STATEMENT: Approved for Public Release;
Distribution Unlimited

The views, opinions and/or findings contained in this report are those of the author(s) and should not be construed as an official Department of the Army position, policy or decision unless so designated by other documentation.

REPORT DOCUMENTATION PAGE				Form Approved OMB No. 0704-0188	
Public reporting burden for this collection of information is estimated to average 1 hour per response, including the time for reviewing instructions, searching existing data sources, gathering and maintaining the data needed, and completing and reviewing this collection of information. Send comments regarding this burden estimate or any other aspect of this collection of information, including suggestions for reducing this burden to Department of Defense, Washington Headquarters Services, Directorate for Information Operations and Reports (0704-0188), 1215 Jefferson Davis Highway, Suite 1204, Arlington, VA 22202-4302. Respondents should be aware that notwithstanding any other provision of law, no person shall be subject to any penalty for failing to comply with a collection of information if it does not display a currently valid OMB control number. PLEASE DO NOT RETURN YOUR FORM TO THE ABOVE ADDRESS.					
1. REPORT DATE September 2015		2. REPORT TYPE Annual		3. DATES COVERED 1 Sep 2014 - 31 Aug 2015	
4. TITLE AND SUBTITLE Characterizing and Targeting Bone Marrow-Derived Inflammatory Cells in Driving the Malignancy and Progression of Childhood Astrocytic Brain Tumors				5a. CONTRACT NUMBER	
				5b. GRANT NUMBER W81XWH-13-1-0303	
				5c. PROGRAM ELEMENT NUMBER	
6. AUTHOR(S) Yujie Huang E-Mail:yuh2005@med.cornell.edu				5d. PROJECT NUMBER	
				5e. TASK NUMBER	
				5f. WORK UNIT NUMBER	
7. PERFORMING ORGANIZATION NAME(S) AND ADDRESS(ES) Cornell University, Weill Cornell Medical College 1300 York Avenue, New York, NY 10065-4805				8. PERFORMING ORGANIZATION REPORT NUMBER	
9. SPONSORING / MONITORING AGENCY NAME(S) AND ADDRESS(ES) U.S. Army Medical Research and Materiel Command Fort Detrick, Maryland 21702-5012				10. SPONSOR/MONITOR'S ACRONYM(S)	
				11. SPONSOR/MONITOR'S REPORT NUMBER(S)	
12. DISTRIBUTION / AVAILABILITY STATEMENT Approved for Public Release; Distribution Unlimited					
13. SUPPLEMENTARY NOTES					
14. ABSTRACT In this study, we have utilized glioma patients along with two unique murine glioma models: RCAS glioma model and Gl261 model to study various lineages of BMDCs during different stages of glial tumors. Importantly, we identified the unique the population VEGFR2+MDSCs in both patients and mice, which might be used as a surrogate marker for glioma diagnosis and prognosis in future. We have validated the changes of myeloid lineage and endothelial lineages during the progression of gliomas, and We observed bone marrow derived mesenchymal stem cells have only minimal effort on tumor progression. We have created inducible VEGFR2 knockout system in RCAS-tva model. We demonstrated that bone marrow derived VEGFR2 signaling plays an important role in myeloid differentiation, and infiltration into tumor tissues. Deficiency of VEGFR2 in BMDCs led to impairment of tumor associated myeloid cells and delayed progression of low-grade glioma. Primary tumor up-regulates VEGFR2 in BMDCs through ID2/E2A pathway. All of these findings may have implications to suppress the switch of low-grade to high-grade transformation, and predict the long-term survival.					
15. SUBJECT TERMS Glioma, Pediatric, bone-marrow-derived-cells, endothelial, mesenchymal, myeloid, hematopoietic, differentiation, malignant, transformation, VEGFR2, ID2.					
16. SECURITY CLASSIFICATION OF:			17. LIMITATION OF ABSTRACT Unclassified	18. NUMBER OF PAGES 36	19a. NAME OF RESPONSIBLE PERSON USAMRMC
a. REPORT Unclassified	b. ABSTRACT Unclassified	c. THIS PAGE Unclassified			19b. TELEPHONE NUMBER (include area code)

Table of Contents

	<u>Page</u>
1. Introduction.....	2
2. Keywords.....	3
3. Overall Project Summary.....	4
4. Key Research Accomplishments.....	20
5. Conclusion.....	21
6. Publications, Abstracts, and Presentations.....	22
7. Inventions, Patents and Licenses.....	22
8. Reportable Outcomes.....	22
9. Other Achievements.....	22
10. References.....	23
11. Training & Professional Development	24
12. Appendices	25

1. Introduction

Brain tumors are most frequent solid cancer among all kinds of childhood cancer. Heterogeneity, invasiveness, and complex microenvironment are making therapies as well as research on astrocytic brain tumor particularly challenging^{1,2}. Low-grade gliomas are curable and most patients could live without further progression and severe condition for many years. However, once the glioma progress to high grade, the quality of life and survival of patients are very poor¹. Based on previous work, we hypothesized the bone marrow derived cells (BMDCs) could serve as a mediator of transition of low grade to high-grade tumor³⁻⁵. The proposed project aims to characterize the various lineages of glioma associated BMDCs including hematopoietic, endothelial, and mesenchymal lineages in both low grade and high grade stages of glioma. Studying the effect on glioma transition from low grade to high grade by depleting distinct populations of bone marrow derived inflammatory cells including monocyte, granulocytes, endothelial progenitors, and mesenchymal progenitors. Dissecting molecular mechanism/signaling of differentiation of glioma associated BMDCs, and screening the key factors or targets through the entire regulatory pathway. It would contribute to develop therapeutic strategies to target a specific population of BMDCs and their subsequent recruitment, in order to suppress the malignant transformation of gliomas. In this project, we have initiated the study of BMDCs with RCAS and Gl261 murine glioma models as well as glioma patients. We also used transgenic tools to deplete certain populations of BMDCs to study functional contribution of BMDCs for glioma progression.

2. Keywords

Glioma, Pediatric, bone-marrow-derived-cells, endothelial, mesenchymal, myeloid, hematopoietic, differentiation, malignant, transformation, Inhibitor of DNA binding protein.

3. Overall Project Summary

The project focuses on studying the microenvironment and functions of bone marrow derived cells within pediatric astrocytic tumor. In this study, two major glioma models will be used to investigate the role of BMDCs primarily. One is a transgenic mouse using the RCAS/Tv-a system created by Holland and Varmus that develops low-grade gliomas which progress to high-grade tumors over the course of twelve weeks^{5,6}. The other model is syngeneic orthotopic glioma model. GL261^{7,8}, a C57/BL6 derived glioma cell line with different markers such as GFP or luciferase, was intracranial injected to C57/BL6 mice to create allograft glioma. In addition, xenograft models with human glioma cell lines are also utilized. Furthermore, we also have used glioma patients' blood samples to analyze various lineages of BMDCs⁹⁻¹².

Task 1. Characterizing the various lineages of glioma associated BMDCs including hematopoietic, endothelial, and mesenchymal lineages in both low grade and high gradestages of glioma. (90% complete)

We have analyzed the myeloid lineage and endothelial lineage of BMDCs in both patients' blood samples and murine glioma models at low-grade or high-grade stage.

1a. Assess the frequency and absolute numbers of circulating BMDCs in glioma patients. Using flow-cytometry of hematopoietic, as well as endothelial and mesenchymal markers, we will investigate whether the frequency of HPCs, VEGFR2+ EPCs and CD105+ MSCs correlates with glioma transformation in patients. Human subjects involve this study will be radiographically-suspected or biopsy prove low-grade astrocytoma (WHO grade I and II) versus histology proven high grade gliomas (WHO grade III and IV). Blood samples will be collected at the time of diagnosis. Subjects selected for this study may be between 2 years and 16 years of age. We plan to enroll 160 human subjects, and quarterly enrollment is 20. The identifications of human subjects will not be accessible for research team, and only information of human subjects that research team is aware of is the patients' diagnosis and diseases' history.

Up to date, we have recruited 107 glioma patients with low-grade or high-grade glioma, plus 26 healthy volunteers as control into this study. Patients or healthy volunteers' peripheral blood has been analyzed with various lineages makers as showed in the figures below:

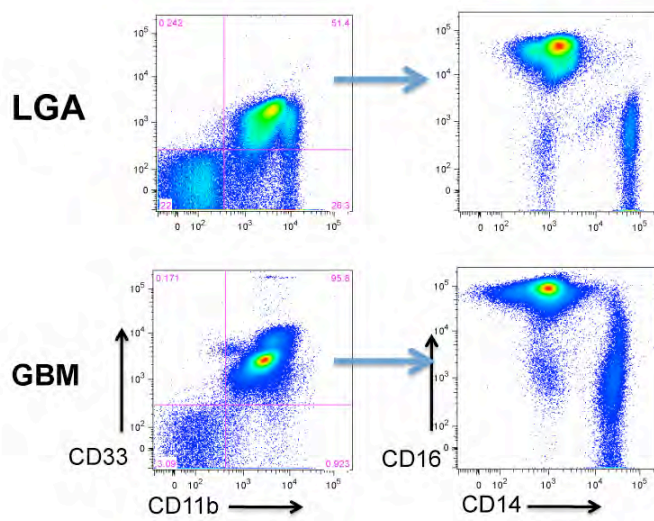


Figure 1. Characterizing myeloid lineage of BMDCs in patients (CD11b, CD33, CD14, and CD16) by flow cytometry in peripheral of low-grade astrocytoma patients (LGA) vs glioblastoma patients (GBM).

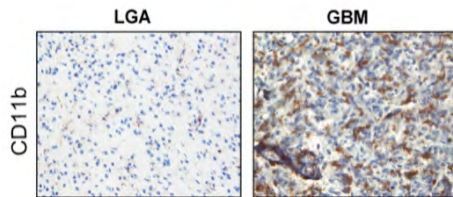


Figure 2. IHC of CD11b (infiltrated myeloid cells) on archived paraffin embedded tumor tissue from low-grade astrocytoma patients (grade II) vs glioblastoma patients (grade IV).

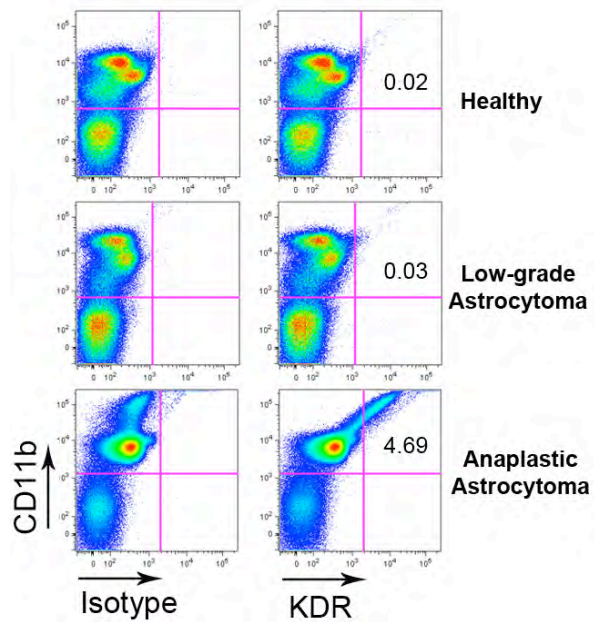


Figure 3. Characterizing endothelial/myeloid lineage of BMDCs in patients by CD11b, KDR (VEGFR2) in peripheral of low-grade astrocytoma patients (LGA), glioblastoma patients (GBM), and healthy volunteers.

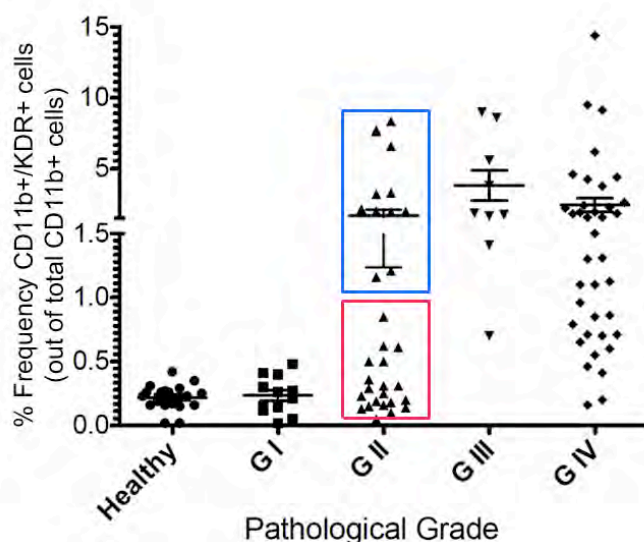


Figure 4. Statistic dots-plot on frequency of CD11b+/VEGFR2(KDR)+ cells out of total CD11b+ cells in patients with different stages of disease. Healthy donor served as a control. GIII/GIV vs healthy, One way ANOVA, $P < 0.001$.

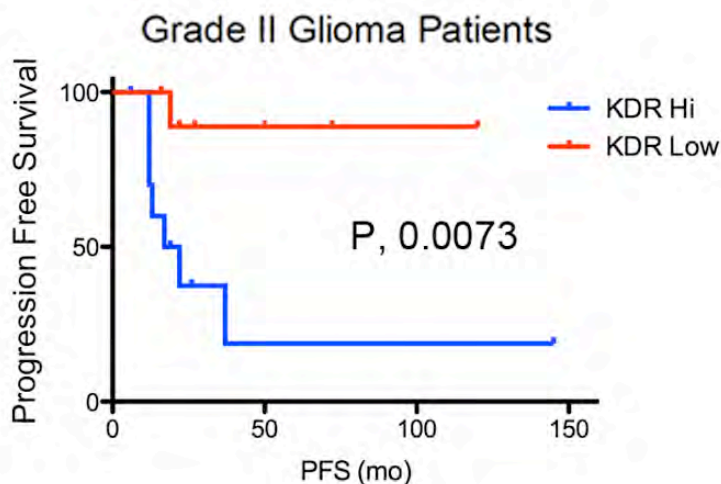


Figure 5. Grade II glioma patients were sub-divided into two groups, based on the frequency of CD11b+/KDR (VEGFR2)+ cells: KDR Hi and KDR Lo (cut-off, 1.0%). Kaplan-Meier curves for progression-free survival over 12 months are presented (27 subjects). $P < 0.01$ by log-rank test.

During the study of BMDCs with glioma patients' blood samples, we have found that the number of myeloid derived support cells (MDSCs) within myeloid lineage increased following the progression of diseases. The MDSCs are heterogeneous regarding the

expression of CD14/CD16, representing monocytic or granulocytic sub-lineages (Figure 1). While the tumor progressed, we also observed more infiltrated myeloid cells within tumor tissues (Figure 2). Interestingly, when we examine the expression of VEGFR2 to study endothelial lineage of BMDCs, we found the majority of VEGFR2 expressing cells are CD11b positive as showed in Figure 3. It suggested that there is overlap or interaction between myeloid lineage and endothelial lineage of BMDCs. Quantification of CD105+/C-kit+ BMDCs indicates no significant difference in MSCs from patients with in low-grade patients vs high-grade patients. Therefore, we would focus on unraveling the role of myeloid/endothelial lineage in glioma progression by following animal study.

Based on the analysis on large cohort of patients, we found that the number of CD11b+/KDR+ BMDCs have significant correlation with the pathological diagnosis of patients. The ratio of KDR+ myeloid cells was significantly higher in blood samples derived from patients with high-grade gliomas when compared with samples from patients with low-grade gliomas. Specifically, the levels of CD11b+KDR+ cells were higher in patients with WHO grade III or IV tumors than it is in patients with grade I tumors and healthy controls (Figure 4). Perhaps most striking is the apparent delineation of two distinct populations of patients, each with pathologically defined grade II astrocytoma. We sub-divided patients with grade II astrocytoma into two subgroups, those with high versus low CD11b+KDR+ values (cut-off of 1.0%). The clinical course and medical histories of the patients were closely followed over 12 months. Disease progression in patients with grade II glioma was assessed by MRI and through subsequent histological diagnoses of grade III or IV glioma. The progression-free survival of our cohort of grade II patients is shown in Fig. 2c. Patients with an elevated percentage of CD11b+KDR+ (KDR Hi) myeloid cells presented a significantly higher likelihood of tumor progression from fibrillary to anaplastic variants (Figure 5).

1b. Evaluate the frequency and number of the same BM-derived populations in blood, bone marrow and metastatic organs of murine models of glioma during low grade, transformation grade and high grade phases. Specifically, we will investigate the mobilization of HPCs, EPCs, and MSCs by flow cytometry.

We have analyzed the HPCs, EPCs, and MSCs in both RCAS and GL261 murine glioma models. The 4~6 weeks post-injection of RCAS model were consider as the low-grade stage, and 6~9 weeks were considered high-grade stage. The GL261 model was considered as high-grade glioma model.

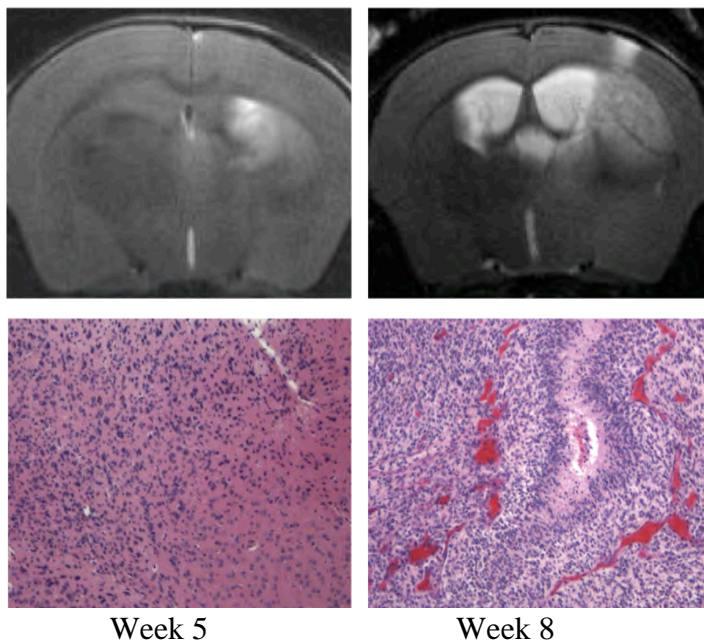


Figure 6. RCAS-tva murine glioma model on low-grade stage (week 5) and high-grade stage (week 8). The MRI or H&E staining from representative mice were showed.

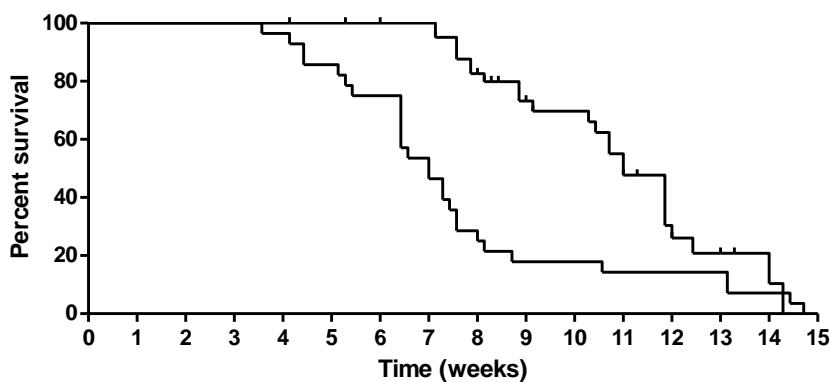


Figure 7. The Kaplan-Meier Survival curves of RCAS-tva tumor bearing mice with or without bone marrow transplantation (BMT). The median survival time for RCAS mice without BMT is 7 weeks, and with BMT is 11 weeks.

We characterized the RCA-tva murine glioma model in our experimental setting, and figured out their low-grade stage and high-grade stage evidenced by MRI and histology. Additionally, we showed the RCAS mice with bone marrow transplantation have delayed progression of tumor, which is important for our next step of study.

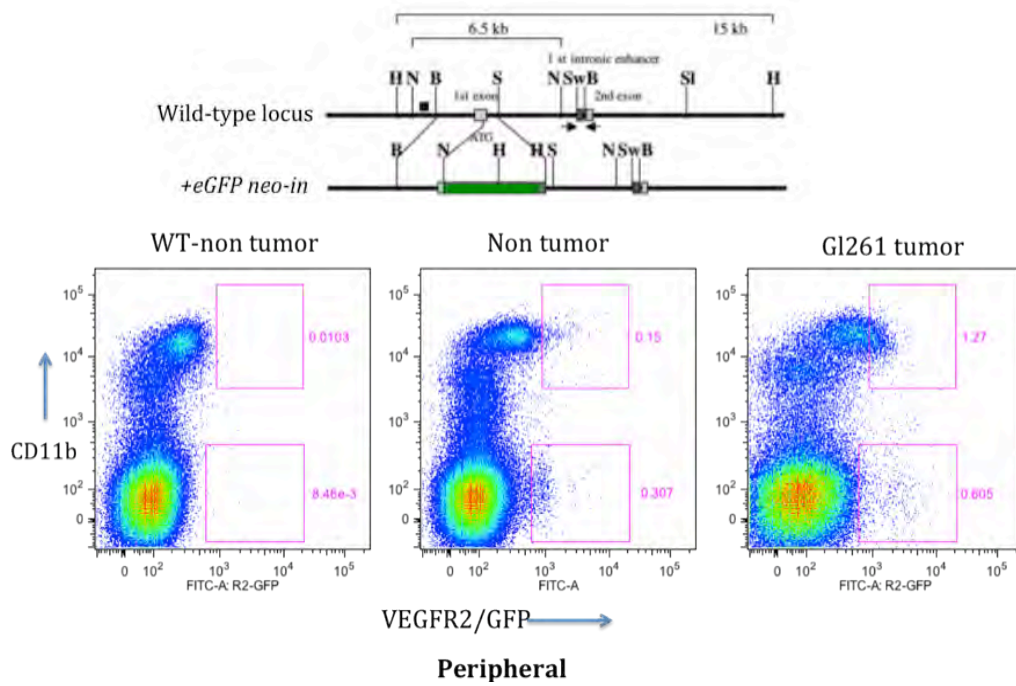


Figure 8. The expression of VEGFR2 on BMDCs in Gl261 model. Upper panel of schematic model showed the VEGFR2-GFP knock in mice for studying expression pattern of VEGFR2. Lower panel of flowcytometry graphs indicate the expression VEGFR2 on CD11b+ or CD11b- population.

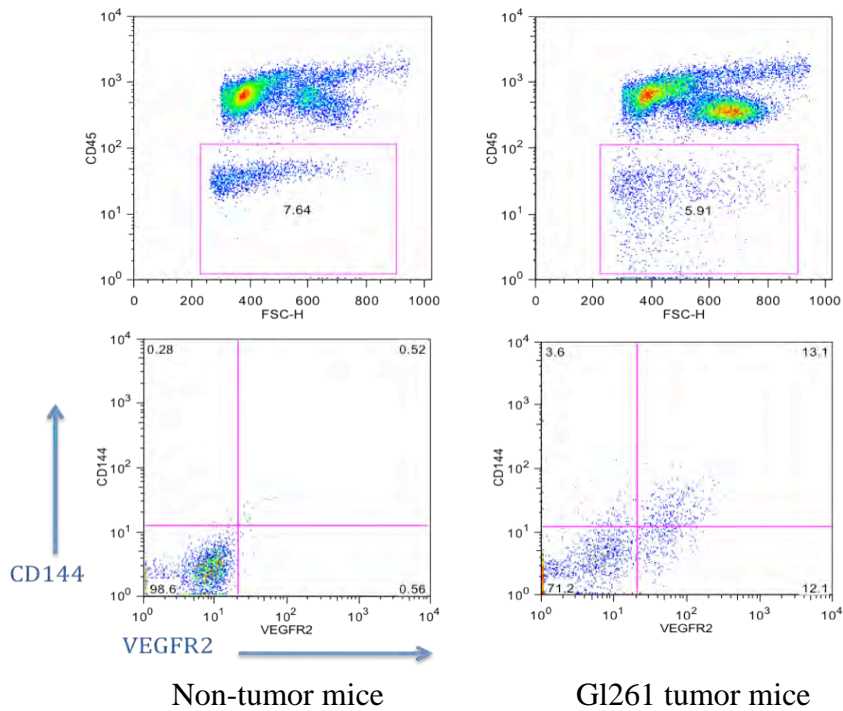


Figure 9. EPC in Gl261 glioma model. Flowcytometry graph of lineage negative CD144+ VEGFR2+ EPC in Gl261 tumor bearing mice.

We have studied the myeloid lineage and EPC with Gli261 glioma model. We observed that both VEGFR2+ myeloid cells and EPCs were elevated by Gli261 tumor, indicating potential interaction of BMDCs differentiation with primary glioma.

Task 2. Studying the effect on glioma transition from low grade to high grade by depleting distinct populations of bone marrow derived inflammatory cells including monocyte, granulocytes, endothelial progenitors, and mesenchymal progenitors. (90% complete)

We have set up all trans-genetic mice lines including ITGAM(CD11b)-DTR/EGFP mice, RosaCreERT2/PDGFR α loxP/loxP mice, and RosaCreERT2/VEGFR2loxP/loxP mice in suitable genetic background for bone marrow transplantation experiments. We performed the lineage depletion experiments with ITGAM(CD11b)-DTR/EGFP and RosaCreERT2/VEGFR2loxP/loxP mice for myeloid or endothelial lineages in both RCAS and Gli261 tumor models.

2a. We plan to transplant the bone marrow from ITGAM(CD11b)-DTR/EGFP mice into the RCAS and Gli261 glioma models, and use diphtheria toxin to induce depletion of myeloid cells in this RCAS glioma model.

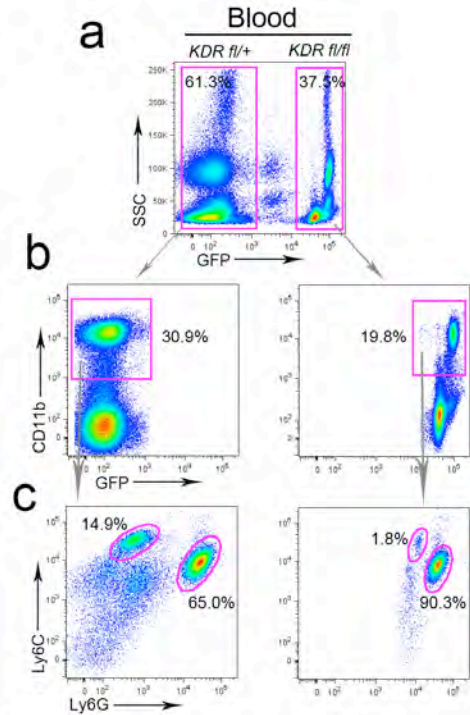


Figure 10. Competitive BMT showed that KDR knockout in bone marrow cells lead to deficiency of the differentiation of monocytic cells. Lethal dose irradiated C57/bl6 mice were transplanted with UBC-GFP/rosa26ERT2-cre/KDRfl/fl and rosa26ERT2-cre/KDRfl/+ bone marrow cells, and Gli261 tumors were implanted after bone marrow engraftment. (a) Peripheral white blood cells were analyzed on SSC and GFP by flow cytometry. The GFP+ and GFP- populations were gated for further analysis. CD11b vs GFP (b), Ly6C vs Ly6G (c).

We have developed the ITGAM(CD11b)-DTR/EGFP bone marrow transplanted mice and implanted mice with G1261 tumor after bone marrow was engrafted. We have tried to deplete the CD11b positive cells in tumor bearing mice once with 5 mice in each group. However, we only obtained approximately 10% deduction of CD11b cells compared with control group. In this case, we didn't see effect on tumor growth. However, as Figure 10 showed, knockout KDR (VEGFR2) led to significant reduction of CD11b+ cells, among of which Ly6 C+ cells were suppressed dramatically. In conclusion, knockout VEGFR2 has considerably effect on myeloid lineage, which is inconsistent co-expression VEGFR2 and CD11b in high-grade patients' BMDCs samples. Accordingly, we have used VEGFR2 deficient model in the following study.

2b. Bone marrow from RosaCreERT2/VEGFR2loxP/loxP mice will be transplanted to both RCAS glioma and G1261 bearing mice to deplete endothelial lineage of bone marrow derived cells by knocking out the VEGFR2 gene. The total number of mice will be used is 30.

We have successfully knockout VEGFR2 in both RCAS model and G1261 murine model. We have studied the effect of VEGFR2 deficiency on glioma progression.

As Figure 11 showed, we could obtain around 90% knocking out efficiency with our RosaCreERT2/VEGFR2loxP/loxP system, without affecting counts of blood cells (CBC) of mice.

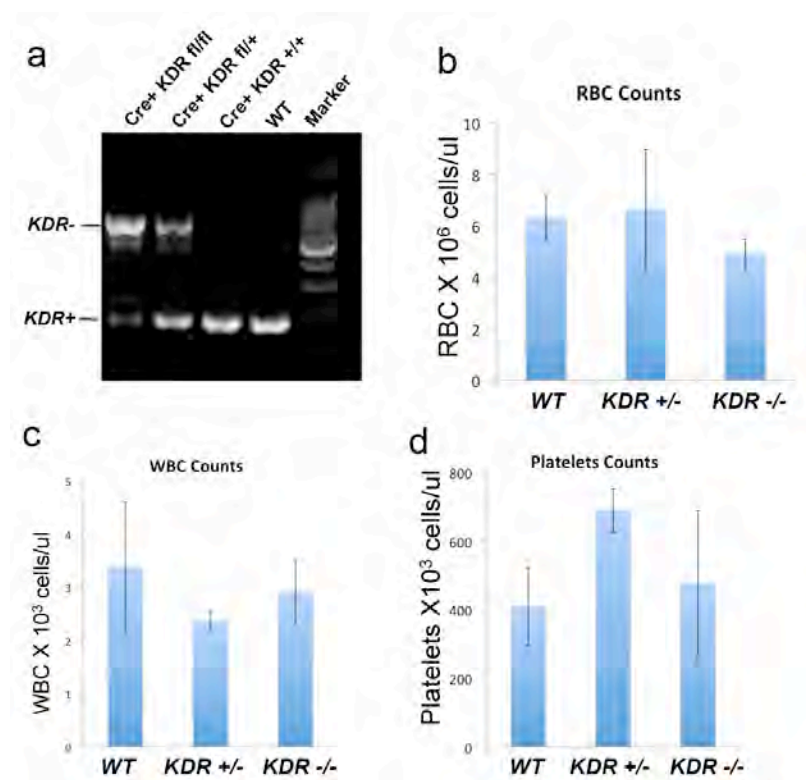


Figure 11. Validation of depletion of VEGFR2 (KDR) allele in bone marrow cells. (a) Amplification of KDR+ or KDR- allele on bone marrow cells of mice bearing indicated genetic background. Tamoxifen was applied to mice one week before testing. Complete blood counts on mice with WT, KDR+/-, or KDR-/- bone marrow (b) Red blood cells, (c) white blood cells, and (d) Platelets.

When we knockout VEGFR2 from BMDCs in Gl261 models, we observed that tumor progression were suppressed as showed in figure 12. In the tumor tissue, we found much less tumor associated myeloid cells (CD11b+) in the VEGFR2 KO group compared with control group (Figure 13). With RCAS system, we found the similar phenotype, after we performed the bone marrow transplantation and induced VEGFR2 knockout, we observed that tumor progression were delayed and median survival time (MST) was significantly elongated (Figure 14).

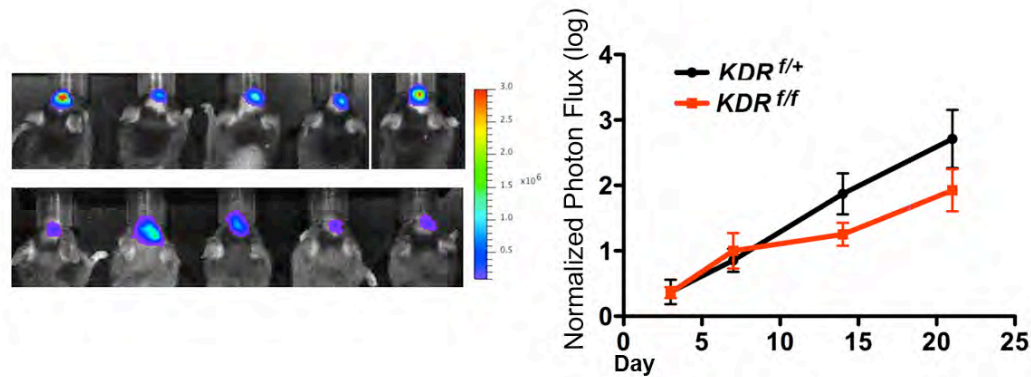


Figure 12. Knocking-out VEGFR2 (KDR) in BMDCs suppress Gl261 tumor growth, tumor-associated myeloid cells, and vasculatures. Chimeric C57/bl6 mice transplanted with rosa26ERT2-cre/KDR^{f1/f1} bone marrow cells (labeled as BM-KDR KO, and BM-KDR control is rosa26ERT2-cre/KDR^{f1/+}) were implanted with luciferase labeled-Gl261 tumors intracranially. Tamoxifen were applied at day 3 post- implantation. The tumors were monitored by bioluminescence. The quantification of bioluminescence based tumor growth.

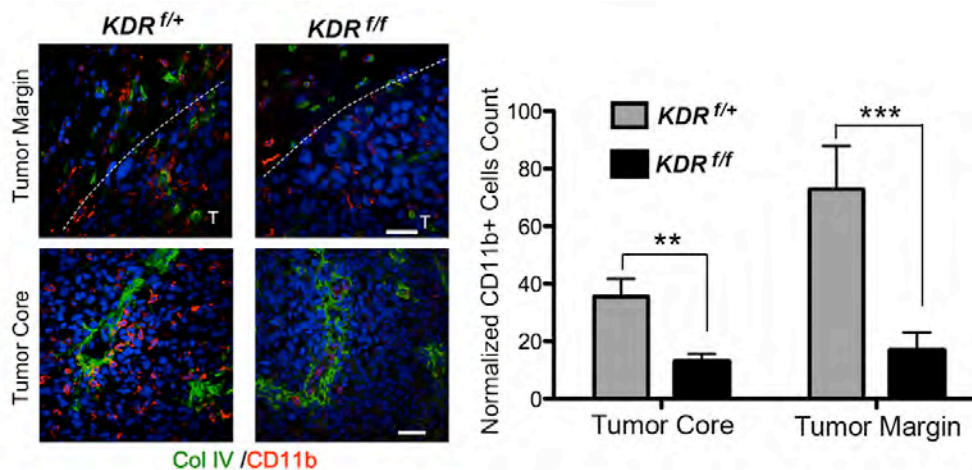
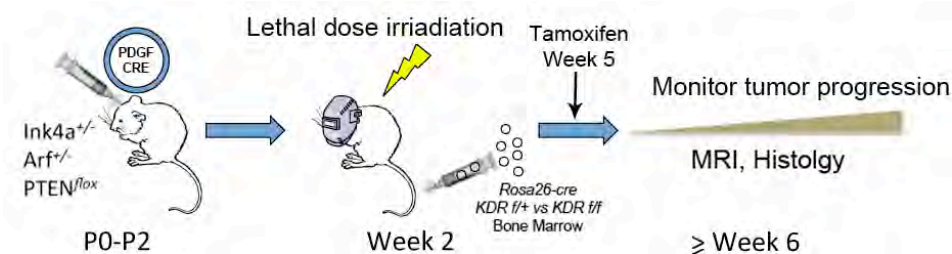


Figure 13. Immuno-staining of vascular basement (Collagen IV) and myeloid cells (CD11b) in the Gl261 tumors from each group. Scale bar, 20 μ m. The number of CD11b cells in tumor core or tumor margin was quantified.



Symptom-free survival of RCAS glioma model

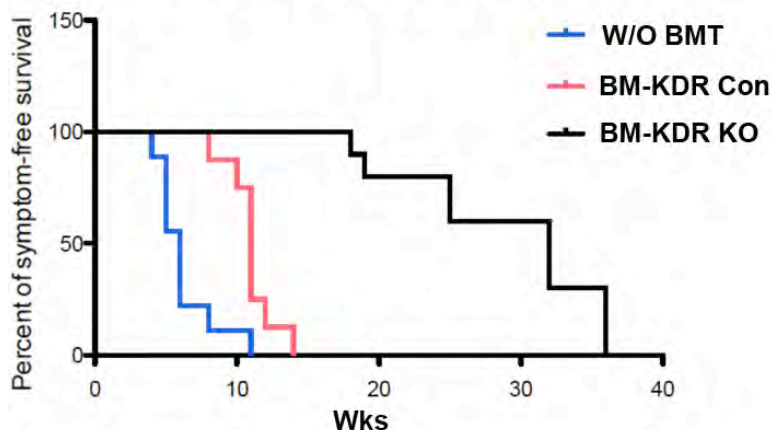


Figure 14. Knocking-out VEGFR2 (KDR) in BMDCs suppress spontaneous malignant transformation of RCAS gliomas. (a) Flow chart of experimental design. Oncogenes were transduced to P0-P2 pups in the beginning. Mice received lethal dose irradiation and received bone marrow transplantation at week 2, and then tamoxifen was applied to mice at week 5 to induce the ablation of target gene. Tumors were monitored by MRI over the process. (b) Kaplan-Meier symptom free survival curve for RCAS mice transplanted with *rosa26ERT2-cre/KDR^{fl/fl}* bone marrow cells (BM-KDR KO), *rosa26ERT2-cre/KDR^{fl/fl}* bone marrow cells (BM-KDR Con), or without irradiation/transplantation (W/O BMT).

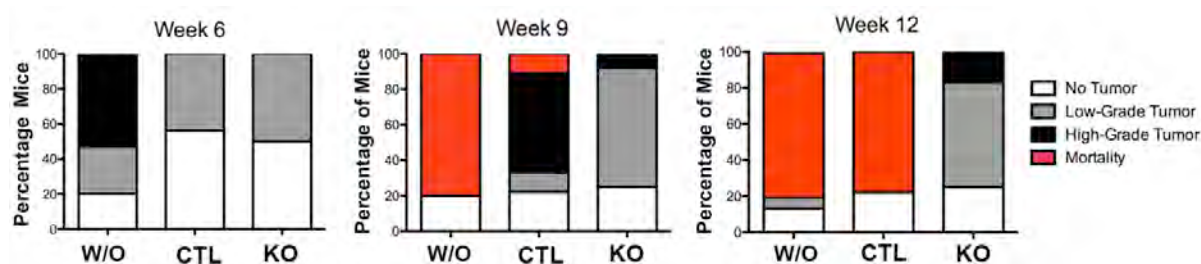


Figure 15. At weeks 6, week 9, and week 12, tumors in each group of mice were assessed and graded based on their MRI and further confirmation with histology. N=19~26.

We compared brain tumors in RCAS/*tva* mice at weeks 6, 9 and 12, utilizing MRI followed by histological examination (Figure 15). Knocking out KDR in BMDCs significantly delayed the malignant transformation of low-grade glioma. By week 9, 60% of RCAS/*tva* mice transplanted with control R26CreERKDR^{fl/+} bone marrow developed high-grade tumors, which had typical malignant features, including robust gadolinium

enhancement on MRI, pseudopalisading necrosis, and microvascular proliferation. In contrast, tumors in 70% of RCAS/tva mice transplanted with R26CreERKDRfl/fl bone marrow remained in the low-grade stage without signs of malignant transformation at week.

2c. Bone marrow cells from RosaCreERT2/PDGFR α loxP/loxP mice will be transplanted to each genetic and orthotopic glioma generating mice. PDGFR α is expressed on bone marrow derived mesenchymal stem cells and PDGF- PDGFR α signal axis is very critical for maintenance of mesenchymal lineage. By knocking out PDGFR α gene, we will study the influence of defection of mesenchymal differentiation on the progression of low-grade glioma. The total number of mice will be used is 30.

We have completed the crossing donor RosaCreERT2/PDGFR α loxP/loxP mice, and the bone marrow transplantation experiments along with tumor study are ongoing. As study has showed, Deletion of PDGFR α gene in BMDCs have no significant influence on development of Gl261 tumor in mice brain. Interestingly, we observed that tumor did growly slower and in RosaCreERT2/PDGFR α loxP/loxP mice compared with control mice. It suggests that residential PDGFR α + cells play more important role in tumor progression than bone marrow derived PDGFR+ cells. (Figure 16)

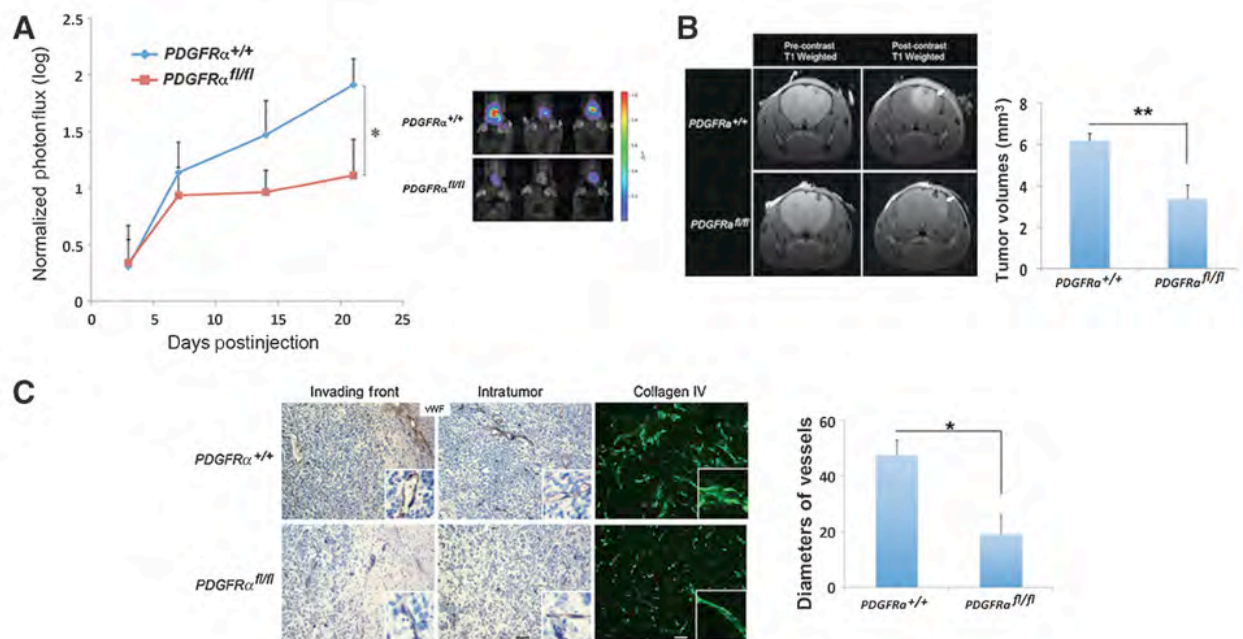


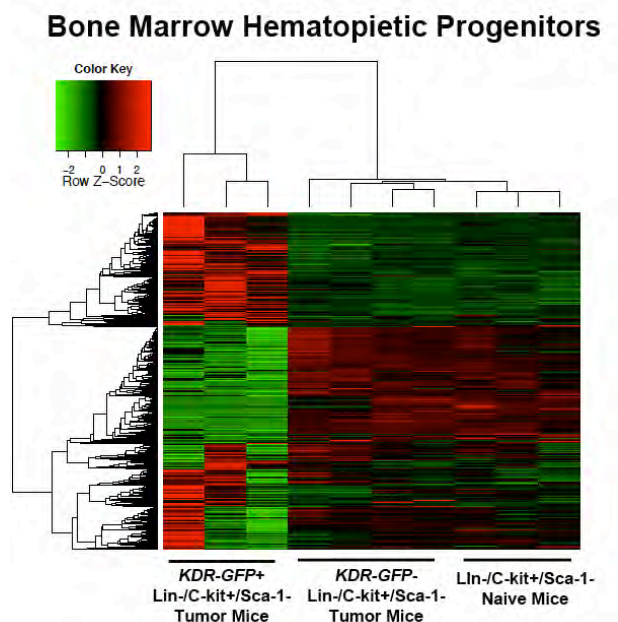
Figure 16. Knocking out PDGFR α in stromal cells inhibits glioma progression. Luciferase-Gl261 cells were intracranially injected into RosaCre-ERT2/PDGFR α fl/fl mice and RosaCre-ERT2/PDGFR α ^{+/+} mice. A, tumor burden is represented by photon flux intensity. $P < 0.05$. B, precontrast and postcontrast T1-weighted MRIs were performed on each group at day 15. Arrows, enhancing tumor. Tumor volume quantification is demonstrated. $P < 0.01$. C, vWF was stained in the tumor periphery and within the tumor of each group (left and middle panels). Collagen IV was stained in each group (right). Scale bar, 50 μ m. Vessel diameters were quantified. $P < 0.05$.

Task 3. Dissecting molecular mechanism/signaling of differentiation of glioma associated BMDCs, and screening the key factors or targets through the entire regulatory pathway. (60% complete)

We will proceed to study which genes in certain lineages of BMDCs could play a critical role in promoting the invasion of glioma. We will isolate specific population from BMDCs from the tumor tissue, blood, and bone marrow. Then we utilize microarray/next generation sequencing, antibody array, LC-TOF-TOF to detect gene and protein expression. To determine the functional contribution of certain genes of interest, or certain subpopulation of BMDCs, we plan to utilize a series of in vitro/in vivo experiments, including basement invasion assay and knock specific genes bone marrow cells and then transplant them into glioma producing mice, to elucidate their specific roles in promoting invasion of glioma cells and infiltration of glioma. Total number of mice will be used for this study is 30.

We have been working on optimizing sorting different lineages of BMDCs by FACS or MACS and tested a few samples by RNA sequencing. The data suggested that ID2/VEGF2 signaling was playing important role in myeloid differentiation.

In order to further delineate the signaling network driving myeloid/endothelial lineage differentiation, we performed gene expression profiling of VEGFR2-expressing hematopoietic progenitor cells (Lin-C-kit+) by mRNA sequencing. Differentially expressed genes from VEGFR2+ versus VEGFR2- HPCs were clustered and arranged in a heatmap. Differentially expressed genes were also clustered and displayed (Figure 17). Candidate genes ($P < 0.05$, > 1.5 -fold change) were divided according to subsets with the highest expression and analyzed for categories with significant enrichment ($P < 0.05$) of categories in Gene Ontology (GO) biologic processes using DAVID tools. Similar categories were grouped accordingly (Figure 18). Inhibitor of DNA binding proteins 2 (ID2) was identified as a significantly up-regulated gene in VEGFR2+ HPCs a strong candidate to be an upstream molecule mediating myeloid endothelial differentiation.



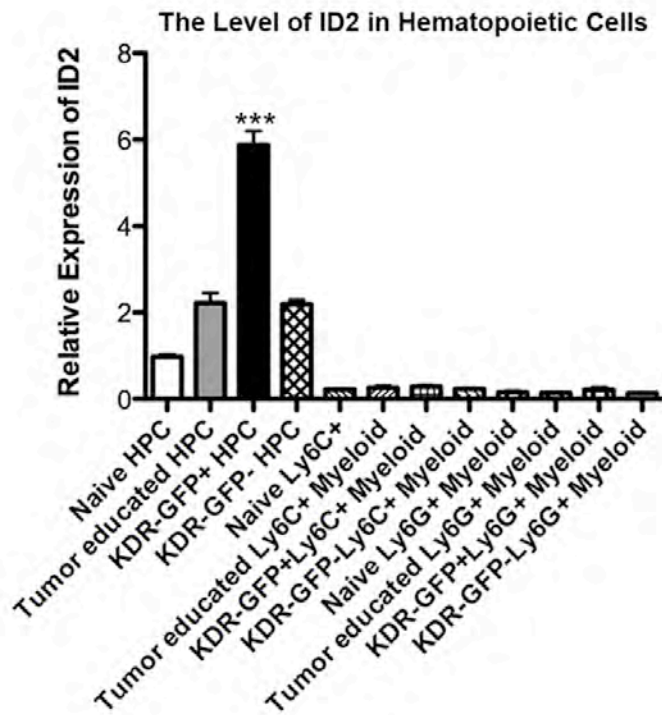


Figure 19. The expression of ID2 in various lineages of hematopoietic cells. Means \pm SEM, *** P < 0.0001 by one way ANOVA.

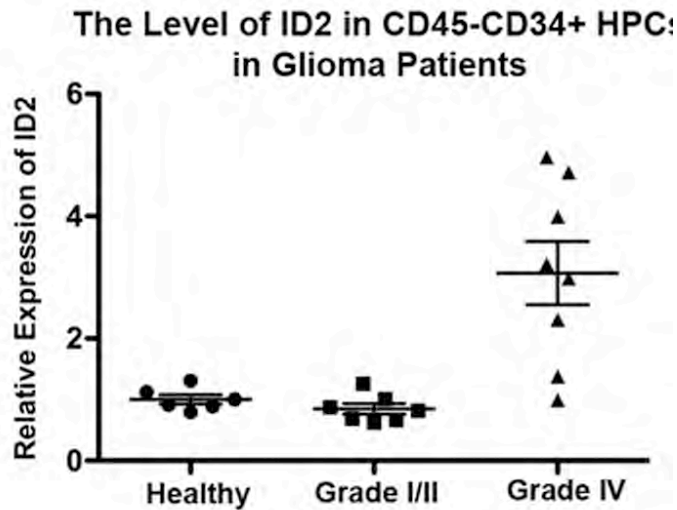


Figure 20. The expression of ID2 in hematopoietic progenitor cells (CD45-CD34+) from patients with low-grade or high-grade gliomas. Means \pm SEM, P < 0.0001 by one way ANOVA.

To validate the up-regulation of ID2 in HPCs, we performed real-time PCR on KDR^{GFP+} HPCs and Ly6C⁺/Ly6G⁺ myeloid cells from tumor-bearing or naïve mice. KDR^{GFP+} HPCs from tumor-bearing mice had higher ID2 levels than KDR^{GFP-} HPCs and HPCs from naïve mice (Figure 19). The expression of ID2 was generally lower in myeloid cells than in HPCs. We also examined the expression of ID2 in glioma patients. HPCs were isolated from healthy controls and patients diagnosed with low-grade and high-grade

gliomas. HPCs from high-grade glioma patients had significantly higher levels of ID2 than did HPCs from healthy controls and low-grade glioma patients ($P < 0.0001$, Figure 20).

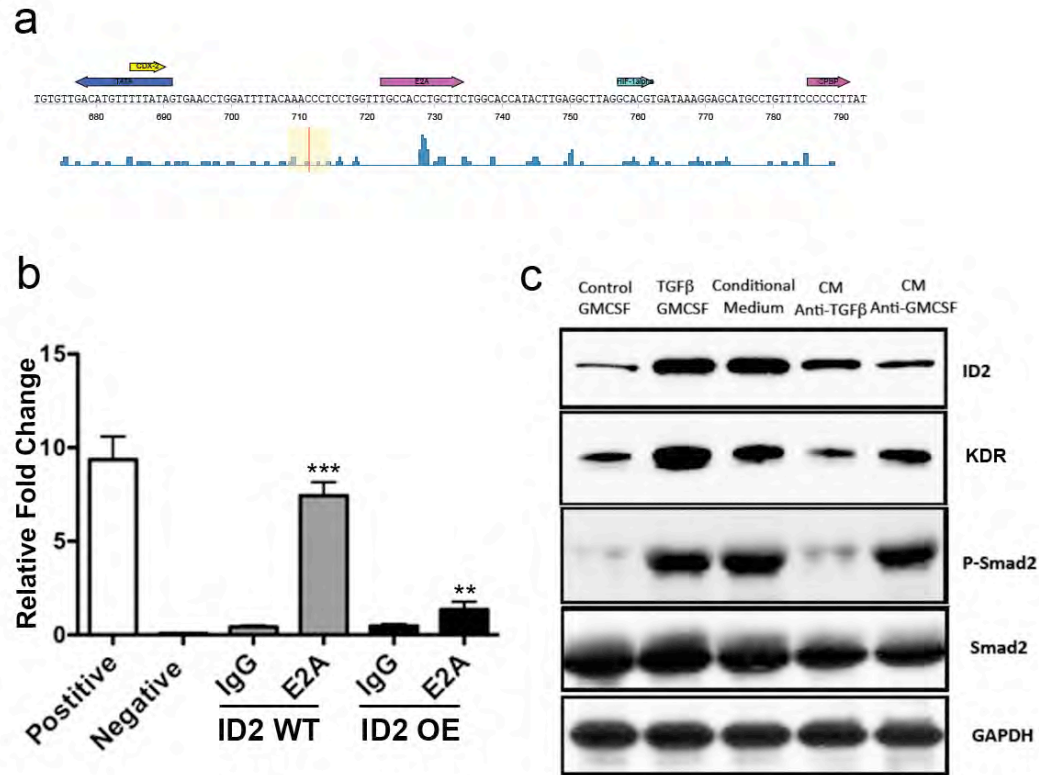


Figure 21. Upstream of KDR (a) the bioinformatic analysis of promoter and 5'-UTR region of KDR by biobase. Highlighted fragment of KDR promoter showed potential binding site for E2A. (b) Chromatin immunoprecipitation of E2A with or w/o over-expression of ID2. Probe on KDR promoter fragments were used. Means \pm SEM, ** $P < 0.01$, *** $P < 0.0001$ by one way ANOVA. (c) Immunoblotting of KDR and ID2 on in vitro cultured Lineage negative bone marrow cells treated with or w/o TGF- β 1 and GMCSF. Phospho-smad2/smard2 indicated activation of related signaling. The immunoblotting has three replicates.

ID2 functions by inhibiting the binding to DNA of E proteins. To investigate whether ID2 interacted with E proteins to regulate cell fate within the myeloid lineage, we analyzed the promoter region plus the 5' untranslated region of KDR for putative E protein binding sites known as E boxes. We identified a putative binding site for E2A (Figure 21a) within the upstream promoter region of the KDR gene. To conclusively establish the ID2/E-protein/KDR interaction, we performed a chromatin immunoprecipitation assay using E2A antibody in ID2 $^{+/+}$, ID2 over-expressing, and ID2 $^{-/-}$ bone marrow cells. As expected, antibody to E2A was able to pull down the upstream fragment of KDR. Over-expression of ID2 abolished the binding of E2A to the promoter of the KDR gene (Figure 21b). Although it was beyond the scope and focus of our analysis, our data suggested that soluble GM-CSF and TGF- β may influence the expression of ID2 within pluri-potential bone marrow populations, regulating KDR expression thereby directing cell fate. GM-CSF and TGF- β induced expression of ID2 and KDR in lineage negative bone marrow cells (Figure 21c) similar to conditioned

medium derived from G1261 cells; blocking either one reversed ID2 and KDR expression. These results support the hypothesis that glioma-secreted GM-CSF and TGF- β initiate pro-tumoral myeloid cell differentiation, directing the formation of the KDR⁺-pro-angiogenic immune cell population, which plays a crucial role in the tumor microenvironment and malignant glioma transformation.

4. Key Research Accomplishments

- I. We have demonstrated that myeloid derived suppressor cells increased following the progression of astrocytic tumor in both patients and murine models.
- II. We identified a specific population across endothelial and myeloid lineages, which is VEGFR2+CD11b+ population in patients and tumor bearing mice.
- III. We successfully performed knock out VEGFR2 within BMDCs in murine glioma models, and observed that bone marrow derived VEGFR2 contribute to tumor progression and animal survival.
- IV. We have performed RNA-sequencing on tumor associated myeloid progenitors, and identified inhibitor of DNA binding proteins 2 was related with pro-tumoral myeloid differentiation.
- V. We have demonstrated that ID2 was up-regulated in tumor primed hematopoietic progenitor cells in both patients' samples and murine models.
- VI. We identified the binding region of E2A in VEGFR2 promoter, which indicates role of complex E2A/ID2 in regulation of VEGFR2 expression.

5. Conclusion

In this study, we have utilized glioma patients along with two unique murine glioma models: RCAS glioma model and GL261 model to study the BMDCs during different stages of glial tumor. Importantly, we identified the unique the population VEGFR2+MDSCs in both patients and mice, which might be used as a surrogate marker for glioma diagnosis and prognosis in future. We have validated the changes of myeloid lineage and endothelial lineages while the progression of gliomas, and observed the increased population of myeloid derived suppressor cells and endothelial progenitor cells in murine glioma models. We have created inducible VEGFR2 knockout system in glioma bearing mice. Taking advantage of this transgenic model, we demonstrated that bone marrow derived VEGFR2 signaling plays an important role in myeloid differentiation, and infiltration into tumor tissues. Deficiency of VEGFR2 in BMDCs led to impairment of tumor associated myeloid cells and delayed progression of low-grade glioma. All of these findings may help to find the approach to suppress the progression of low-grade glioma into high-grade form, and have implications to predict the long-term survival of glioma patients^{13,14}.

In the following study, we will keep exploring the various lineages of BMDCs in both low-grade and high-grade glioma patients. We would further validate functional role of VEGFR2+ BMDCs in malignant transformation, and investigate the connection of myeloid differentiation with tumor associated macrophages/neutrophils. We would dedicate our effort to delineate the signaling pathways, which affect pro-tumoral myeloid cells, and further characterize the downstream signaling of inhibitor of DNA binding proteins 2 m(ID2) in BMDCs^{15,16}. The up-regulation of ID2 in hematopoietic progenitors provided insight how tumor enhances VEGF signaling in pro-tumoral differentiation via ID2/E2A complex.

6. Publications, Abstracts, and Presentations

1) Abstract/Oral presentation

ID2/KDR drives the differentiation of pro-malignant myeloid derived suppressor cells in glioma. Yujie Huang, Prajwal Rajappa, Jacqueline Bromberg, David Lyden, Jeffrey Greenfield. Cold Spring Harbor-Asia Meeting (International) "FRONTIERS OF IMMUNOLOGY IN HEALTH & DISEASES" September 2–September 6, 2014

ID2/KDR drives formation of pro-malignant myeloid derived suppressor cells in glioma. Yujie Huang, Prajwal Rajappa, Jacqueline Bromberg, David Lyden, Jeffrey Greenfield. Annual Scientific Meeting of the Society for Neuro-Oncology, November 13-16, 2014

Oligodendrocyte progenitor cells promote neovascularization in glioma by disrupting the blood-brain barrier. Huang Y, Hoffman C, Rajappa P, Kim JH, Hu W, Huse J, Tang Z, Li X, Weksler B, Bromberg J, Lyden DC, Greenfield JP. Cancer Research. 2014 15;74(4):1011-21.

7. Inventions, Patents and Licenses

None

8. Reportable Outcomes

None

9. Other Achievements

None

10. References

1. Louis, D.N., *et al.* The 2007 WHO classification of tumours of the central nervous system. *Acta Neuropathol* **114**, 97-109 (2007).
2. Huse, J.T. & Holland, E.C. Targeting brain cancer: advances in the molecular pathology of malignant glioma and medulloblastoma. *Nat Rev Cancer* **10**, 319-331 (2010).
3. Kaplan, R.N., *et al.* VEGFR1-positive haematopoietic bone marrow progenitors initiate the pre-metastatic niche. *Nature* **438**, 820-827 (2005).
4. Joyce, J.A. & Pollard, J.W. Microenvironmental regulation of metastasis. *Nat Rev Cancer* **9**, 239-252 (2009).
5. Fomchenko, E.I., *et al.* Recruited Cells Can Become Transformed and Overtake PDGF-Induced Murine Gliomas In Vivo during Tumor Progression. *Plos One* **6**(2011).
6. Shih, A.H., *et al.* Dose-dependent effects of platelet-derived growth factor-B on glial tumorigenesis. *Cancer Res* **64**, 4783-4789 (2004).
7. Newcomb, E.W., *et al.* Flavopiridol inhibits the growth of GL261 gliomas in vivo: implications for malignant glioma therapy. *Cell Cycle* **3**, 230-234 (2004).
8. Newcomb, E.W., *et al.* Antiangiogenic effects of nescapine enhance radioresponse for GL261 tumors. *Int J Radiat Oncol Biol Phys* **71**, 1477-1484 (2008).
9. Fridlender, Z.G., *et al.* Polarization of Tumor-Associated Neutrophil Phenotype by TGF-beta: "N1" versus "N2" TAN. *Cancer Cell* **16**, 183-194 (2009).
10. Gabrilovich, D.I. & Nagaraj, S. Myeloid-derived suppressor cells as regulators of the immune system. *Nat Rev Immunol* **9**, 162-174 (2009).
11. Gordon, S. & Taylor, P.R. Monocyte and macrophage heterogeneity. *Nat Rev Immunol* **5**, 953-964 (2005).
12. Greenfield, J.P., *et al.* Surrogate Markers Predict Angiogenic Potential and Survival in Patients with Glioblastoma Multiforme. *Neurosurgery* **64**, 819-826 (2009).
13. Shojaei, F., *et al.* Tumor refractoriness to anti-VEGF treatment is mediated by CD11b+Gr1+ myeloid cells. *Nat Biotechnol* **25**, 911-920 (2007).
14. Pyonteck, S.M., *et al.* CSF-1R inhibition alters macrophage polarization and blocks glioma progression. *Nat Med* **19**, 1264-+ (2013).
15. Li, H.J., Ji, M., Klarmann, K.D. & Keller, J.R. Repression of Id2 expression by Gfi-1 is required for B-cell and myeloid development. *Blood* **116**, 1060-1069 (2010).
16. Kee, B.L. E and ID proteins branch out. *Nat Rev Immunol* **9**, 175-184 (2009).

11. Training & Professional Development

In the past two year, I have received extensive trainings and related proceedings from various workshops, meetings, and hands-on practices, in addition to regular mentorships form weekly lab meeting and journal club. To follow the frontiers of tumor immunology and tumor microenvironment research, I have attended a workshop on tumor microenvironment (TME) organized by national cancer institute in April 2014. I have communicated several renowned experts on TME with their study and our proceedings. I also delivered a talk about our work in Cold Spring Harbor-Asia meeting focusing on immunology in diseases, and it was well received. In November 2014, my abstract on protumora myeloid differentiation was selected for oral presentation on Annual Meeting of Society of Neuro-Oncology. Part of my research on PDGF signaling contributed to a publication on Cancer Research in 2014. Additionally, to update my knowledge on biomedical and genomic fields, I have continued courses and workshops including “Genomic workshop”, “Next generation sequencing analysis”, and “Biostatics for Clinical Studies”, which are provided by Clinical Translational Science Center in Weill Cornell Medical College. All the training opportunities armed me for better bench-side research and long-term career development. According to the feedback from my presentations and publications, our work has been well received by scientific community. I am confident to achieve the career goal that I set in the original proposal.

Appendices

Oligodendrocyte Progenitor Cells Promote Neovascularization in Glioma by Disrupting the Blood–Brain Barrier

Yujie Huang^{1,4}, Caitlin Hoffman^{1,4}, Prajwal Rajappa^{1,4}, Joon-Hyung Kim^{1,4}, Wenhao Hu⁵, Jason Huse⁵, Zhongshu Tang⁷, Xuri Li⁷, Babette Weksler³, Jacqueline Bromberg⁶, David C. Lyden^{2,4}, and Jeffrey P. Greenfield^{1,4}

Abstract

Enhanced platelet-derived growth factor (PDGF) signaling in glioma drives its development and progression. In this study, we define a unique role for stroma-derived PDGF signaling in maintaining tumor homeostasis within the glioma microenvironment. Large numbers of PDGF receptor- α (PDGFR α)-expressing stromal cells derived from oligodendrocyte progenitor cells (OPC) were discovered at the invasive front of high-grade gliomas, in which they exhibited a unique perivascular distribution. In PDGFR α -deficient host mice, in which orthotopic GL261 tumors displayed reduced outgrowth, we found that tumor-associated blood vessels displayed smaller lumens and normalized vascular morphology, with tumors in host animals injected with the vascular imaging agent gadolinium also being enhanced less avidly by MRI. Notably, glioma-associated OPC promoted endothelial sprouting and tubule formation, in part by abrogating the inhibitory effect that perivascular astrocytes exert on vascular endothelial junctions. Stromal-derived PDGF-CC was crucial for the recruitment and activation of OPC, insofar as mice genetically deficient in PDGF-CC phenocopied the glioma/vascular defects observed in PDGFR α -deficient mice. Clinically, we showed that higher levels of PDGF-CC in glioma specimens were associated with more rapid disease recurrence and poorer overall survival. Our findings define a PDGFR α /PDGF-CC signaling axis within the glioma stromal microenvironment that contributes to vascular remodeling and aberrant tumor angiogenesis in the brain. *Cancer Res*; 74(4); 1011–21. ©2013 AACR.

Introduction

The tumor microenvironment is a complex amalgam of tumor cells, intermingling parenchymal cells, infiltrating immune system cells, and a vascular network of endothelial cells, which in concert determine the pathologic and biological features of distinct tumors. Cancer diagnoses and grades significantly vary the composition of the tumor microenvironment (1–3). Gliomas, malignancies arising from glial cells within the central nervous system (CNS), harbor multiple cell types in addition to cells with tumorigenicity. During normal develop-

ment of the CNS, proliferation, differentiation, and migration of glial cells are tightly controlled and well described (4, 5). However, comparatively little is known about the composition, features, and functions of nontransformed glial cells and neural progenitor cells within the natural progression of glioma.

The involvement of platelet-derived growth factor receptor- α (PDGFR α) in gliomagenesis has been well demonstrated (6). Upregulated PDGF signaling through PDGFR α has been found to be a common feature of low-grade astrocytic and oligodendroglial tumors along with a significant subset of glioblastoma multiforme (7, 8). Interestingly, the adult brain contains a widely distributed, abundant progenitor population known as oligodendrocyte precursor cells (OPC), which have been suggested to have high tumor-initiating potential (9–12). These cells identified by expression of NG2/Olig2 are normally cycling and express PDGFR α in postnatal brains (13, 14). Enhanced PDGF signaling is present in a specific population of gliomas (15), suggesting that OPCs might become activated and undergo specific adaptations in response to unique tumor microenvironment conditions. In this study, we explore the distribution and possible functional contributions of OPCs to the vascular microenvironment dependent on PDGFR α /PDGF-CC signaling during glioma progression. We suggest a role for PDGFR α ⁺ OPCs in the destabilization of vascular architecture and integrity as a major functional contributor to tumor angiogenesis and tumor-grade progression.

Authors' Affiliations: ¹Department of Neurological Surgery, The Childhood Brain Tumor Project; ²Department of Pediatrics; ³Division of Hematology–Medical Oncology; ⁴Pediatric Brain Tumor Research, Children's Cancer and Blood Foundation Laboratories, Weill Cornell Medical College; Departments of ⁵Pathology and ⁶Medicine, Memorial Sloan-Kettering Cancer Center, New York, New York; and ⁷National Eye Institute, NIH, Bethesda, Maryland

Note: Supplementary data for this article are available at Cancer Research Online (<http://cancerres.aacrjournals.org/>).

Corresponding Authors: David C. Lyden, 515E 71st Street, New York, NY 10021. Phone: 212-746-3941; Fax: 212-746-8423; E-mail: dcl2001@med.cornell.edu; and Jeffrey P. Greenfield, 525E 68th Street, New York, NY 10065. Phone: 212-746-2363; Fax: 212-746-7729; E-mail: jgreenf@med.cornell.edu

doi: 10.1158/0008-5472.CAN-13-1072

©2013 American Association for Cancer Research.

Materials and Methods

Cells lines and mice lines

PDGF-C-deficient mice have been previously described (16). C57BL/6-derived glioma cells, GL261 (authenticated as Supplementary Table S1) and KR158, were as described previously (17–19). HCMEC/D3 have been previously described (20; additional information available in Supplementary Methods).

Intracranial injections and tumor imaging

The intracranial injections have been described previously (21). Bioluminescence IVIS-100 (Xenogen) and MRI (Bruker Biospin) were performed to monitor the progression of tumor. Tumor margins in each MRI slice were manually outlined. The area of each region of interest was calculated and then multiplied by the slice thickness. All slice volumes were added up to calculate the volume of each three-dimensional (3D) tumor. For detailed methods, please refer to Supplementary Methods.

Adoptive bone marrow transplantation

Transplantation was carried out as previously described (22) with slight modifications. Recipient mice were lethally irradiated with a single dose of 9.5 Gy to their whole body with their heads shielded. Twenty-four hours after irradiation, 5×10^6 total bone marrow cells were injected by tail vein followed by 6 weeks to allow for engraftment of bone marrow cells. The engraftment was confirmed by complete blood count and flow cytometry to ensure adequate hematopoiesis.

Dextran infusion assay

10 mg/mL of 70-kD rhodamine-conjugated Dextran (lysine fixable) was intravenously injected into mice (100 μ L/mouse) as previously described (23). Two hours after dextran injection, mice were perfused with 10 mL PBS followed by perfusion of 5 mL of 4% paraformaldehyde. Brain tissue was dissected and fixed for the subsequent staining.

Microarray analysis

Microarray data can be accessed from Gene Expression Omnibus (NCBI/GEO) under accession number GSE38283. For detailed procedures of the preparation of samples, please refer to Supplementary Methods.

Quantification

All data are given as mean \pm SD or \pm SEM. Differences were compared using Student *t* tests or one-way ANOVA followed by *post hoc* tests. For more experimental procedures and quantification details, please refer to Supplementary Methods.

Results

Stromal cells in glioma express PDGFR α

PDGF signaling is upregulated in many patients with glioma; 30% of patients harboring high-grade gliomas express an amplified or mutated PDGFR α gene (7). The infiltration of bone marrow-derived cells (BMDC) is also considered as a hallmark of tumor progression (22, 24). To better understand the temporal and spatial variation within the glioma micro-

environment of PDGFR α -expressing cells and inflammatory BMDCs, PDGFR α staining was performed on orthotopic GL261 (murine-derived glioma cell line) tumors in mice, which had previously been adoptively transplanted with GFP bone marrow. Large numbers of BMDCs and PDGFR α ⁺ cells were identified at the tumor periphery (Fig. 1A). The number of these peritumoral PDGFR α ⁺ cells increased at day 14 along with the enhanced infiltration of BMDCs (Fig. 1B). We demonstrated that most PDGFR α ⁺ cells, located in the invasive front, were actually nontumor cells. We used orthotopic glioma models with both murine-derived GL261 cells (PDGFR α ⁺) constitutively expressing GFP, as well as human-derived U87-MG and U251 cells also expressing GFP (Fig. 1C and Supplementary Fig. S1A), to show that these were not invading tumor cells. Flow cytometry performed upon whole tumor explants confirmed that PDGFR α -expressing cells are GFP negative in all of the GL261, U87-MG, U251, and KR158 glioma models (Fig. 1D and Supplementary Fig. S1). The existence of peritumoral PDGFR α -expressing cells was also verified in the KR158 glioma model (Supplementary Fig. S1D). Western blot analyses showed enhanced expression of PDGFR α in the tumor margin, compared with tissue isolated from the tumor core, the contralateral hemisphere, or from normal age-matched adult mouse brain (Fig. 1E). Immunostaining of PDGFR α showed more PDGFR α ⁺ cells in tumor periphery than in the contralateral tissue (Supplementary Fig. S2B). Taken together, these results demonstrate that large numbers of PDGFR α stromal cells accumulate in the periphery and invade the front of gliomas.

PDGFR α ⁺ stromal cells derive from OPC and predominate perivascularly

Different tumors are supported by unique microenvironments containing distinct and specific stromal cell populations. To better define the origin of PDGFR α ⁺ stromal cells, we studied the localization of PDGFR α within GL261 tumor specimens using other lineage markers commonly encountered within the glioma microenvironment. PDGFR α ⁺ stromal cells did not express markers of neural stem cells (nestin), astrocytes (glial fibrillary acidic protein, GFAP), or endothelium (collagen IV), nor did they colocalize with BMDCs, identified using GFP after GFP⁺ bone marrow transplant (Supplementary Fig. S2). PDGFR α ⁺ cells did, however, colocalize with NG2, a marker for OPCs. Moreover, PDGFR α ⁺ cells display ramified processes, highly suggestive of OPC morphology, and expressed oligodendrocytic lineage marker Olig2 (Fig. 2A and Supplementary Fig. S2C). PDGFR α ⁺ glioma-associated OPCs (GA-OPC) can be identified adjacent to vascular endothelium in a sandwich-like configuration (Fig. 2B). Because of permeable features of tumor endothelium and the resolution of microscopy, we did observe limited overlaps between CD31/PDGFR α . The GA-OPCs do not, however, colocalize with pericytes (PDGFR β ⁺) or perivascular astrocytes (GFAP⁺; Fig. 2C and D). In addition to their abundance within the tumor periphery, OPCs also exist within tumor cores with perivascular processes as shown by NG2-DsRed (Supplementary Fig. S2D). NG2 is generally used as OPC maker in CNS, but it also marks certain pericytes and microglial cells.

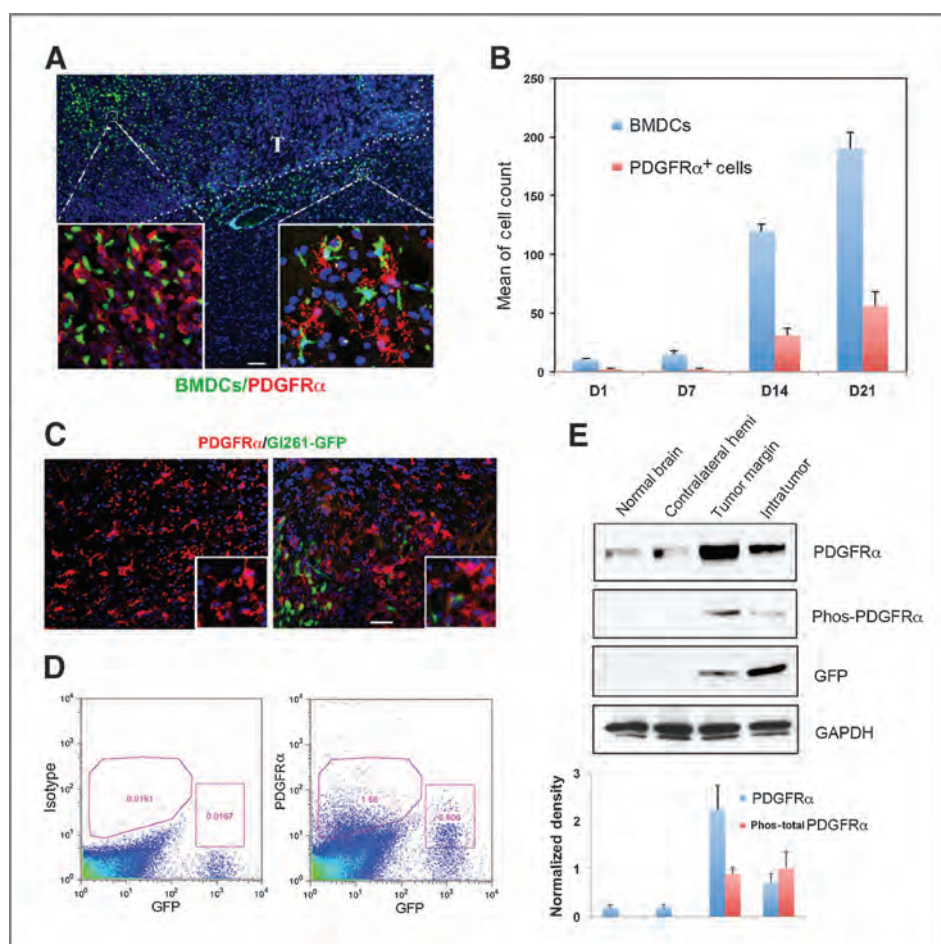


Figure 1. Stromal cells express PDGFR α . A, PDGFR α was stained in Gli261 tumors. PDGFR α ⁺ cells (red) and GFP⁺ BMDCs (green) are shown (left, tumor center; right, tumor periphery). Scale bar, 100 μ m, $n = 4$ mice. B, Gli261 tumors in C57BL/6 mice (GFP⁺ BMDCs) were harvested at D1, D7, D14, and D21 postinjection. The number of PDGFR α cells and GFP⁺ BMDCs in the tumor periphery was quantified (cell count per field). Means \pm SD, $n = 5$ mice. Cell counts in D14 and D21 were significantly higher than those in D1 and D7. $P < 0.001$ by one-way ANOVA. C, PDGFR α was stained (red) in GFP-Gli261 (green) tumors (day 21). Tumor periphery (left) and invasive tumor margin (right) are shown. Scale bar, 50 μ m. D, flow cytometry was performed on dissociated cells from GFP-Gli261 tumors with isotype IgG (left) and PDGFR α antibody (right). E, tissues from tumor core, tumor margin, contralateral hemisphere, and normal adult murine brain were blotted by PDGFR α and phos-PDGFR α . GFP and GAPDH were used as loading controls with tumor cells expressing GFP. Normalized densitometric analyses on three independent experiments ($n = 3$ mice) were provided below each lane. The level of PDGFR α in tumor margin is significantly higher than those in other groups ($P < 0.001$) by one-way ANOVA.

PDGFR α ⁺ stromal cells facilitate the progression and neovascularization of glioma

Tumor cells may educate adjacent nontransformed cells into forming tumor-associated stroma, which can be differentiated from the normal tissue (3, 25). In response to malignancy, OPCs may be activated through PDGFR α signaling (9, 26). To understand the functional role of GA-OPCs in the progression of glial malignancies, we created an orthotopic and syngeneic model using Gli261 cells transfected with a luciferase gene. These cells were implanted in PDGFR α -knockout mice to study the importance of PDGFR α signaling between stromal and tumors cell populations, upon glioma progression. In *Rosa-cre/PDGFR α ^{fl/fl}* mice, growth of Gli261 tumors was inhibited compared with tumor growth in *Rosa-cre/PDGFR α ^{+/+}* mice (Fig. 3A). MRI analysis of Gli261 tumors in *PDGFR α ^{fl/fl}* mice demonstrated animals with less tumor burden and tumors

with less contrast enhancement on MRI than tumors within control mice (Fig. 3B). Compared with tumors in *PDGFR α ^{+/+}* mice, tumors in *PDGFR α ^{fl/fl}* mice had a slightly higher blood vessel density (Supplementary Fig. S3A) and demonstrated distinct vascular morphology. Gliomas within *PDGFR α ^{fl/fl}* mice demonstrated considerably smaller diameters of vessel lumens (Fig. 3C), similar to vasculature typical within the normal mouse brain. Importantly, within *PDGFR α ^{fl/fl}* mouse tumors, pericyte density and architecture was not significantly changed from *PDGFR α ^{+/+}* mice as visualized by the staining for PDGFR β (Supplementary Fig. S3B).

Neovascularization of gliomas is distinct from other types of tumors. Perhaps due to the brain's robust vascular network, brain tumors either remodel preexisting blood vessels or recruit endothelial progenitor cells to undergo microvascular proliferation, a hallmark of high-grade gliomas (1, 27).

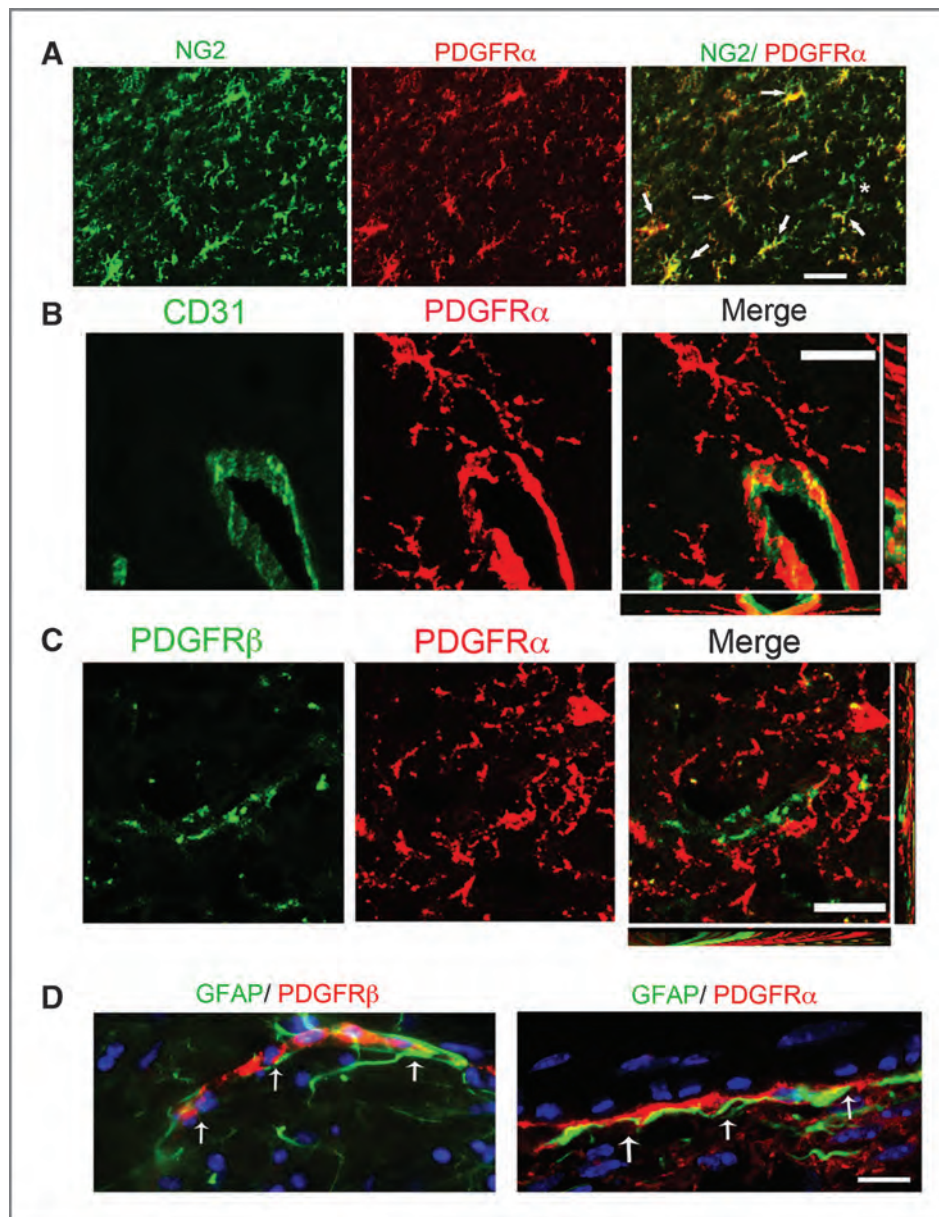


Figure 2. OPC-derived PDGFR α stromal cells are perivascular. **A**, PDGFR α (red) colocalizes with NG2 (green) in the tumor periphery. Arrow, overlap. Asterisk, NG2⁺ cells (green) with suggestive pericyte morphology. Scale bar, 50 μ m. **B**, PDGFR α is adjacent to blood vessel marker CD31 and is not colocalized with the pericyte marker PDGFR β (**C**). Z-stack imaging was used with confocal microscopy. Scale bar, 20 μ m. **D**, costaining of GFAP (perivascular astrocytes) and PDGFR β (pericytes) on Gli261 tumor periphery. Arrows, vascular lumens; scale bar, 20 μ m.

Compared with normal brain and low-grade gliomas, grade III and IV gliomas have distorted, enlarged blood vessels but do not necessarily demonstrate higher blood vessel density (27). Blood vessels in high-grade gliomas are distinguishable from those in low-grade gliomas not by their density, but by their morphology. In *PDGFR α ^{fl/fl}* mice, Gli261 brain tumor-associated blood vessels were not enlarged or distorted compared with that within tumors in wild-type mice. Tumor cells in *PDGFR α ^{fl/fl}* mice have less mitotic activity (decreased Ki67 staining), less hypoxia demonstrated (decreased pimonidazole staining), and less leakiness as indicated by a dextran infusion assay (Supplementary Fig. S3C). Other factors, which could theoretically induce changes in vascular morphology, were studied in both groups of animals by measuring the infiltration of BMDCs and monitoring hematopoiesis; there were moder-

ate decreases of infiltrating BMDCs within Gli261 tumors in *PDGFR α ^{fl/fl}* mice (Supplementary Fig. S4A), and hematopoiesis does not appear to be affected (Supplementary Fig. S4B).

GA-OPCs facilitate angiogenesis

To better understand the contribution of GA-OPCs to the vascular remodeling occurring during glioma neovascularization, we performed *in vitro* assays using primary GA-OPCs cultures. Primary human-derived GA-OPCs and glioma cells were isolated directly from glioma resections (Supplementary Fig. S5A); OPCs were maintained in the progenitor stage within the oligodendritic lineage (Supplementary Fig. S5B and S5C). Using a 3D culture system, we cocultured human brain endothelial cells (HCEC/D3) with GA-OPCs or human astrocytes, or both, to study their interactions. We labeled the HCEC/D3

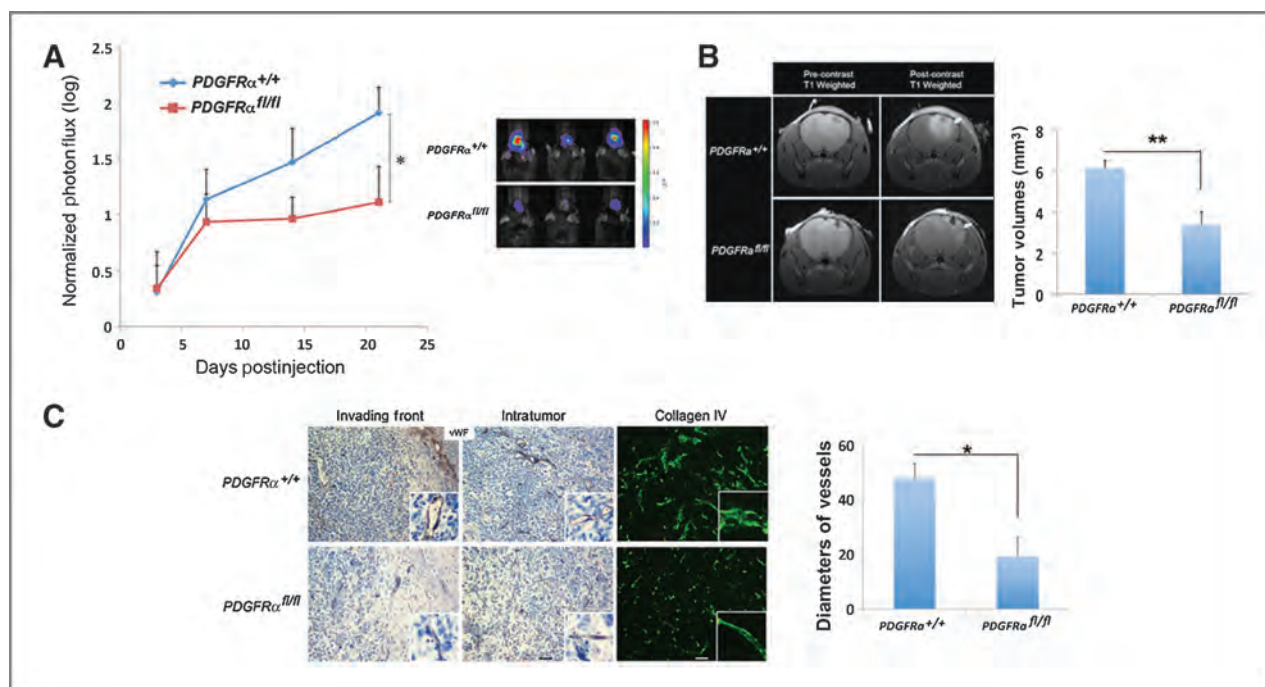


Figure 3. Knocking out PDGFR α in stromal cells inhibits glioma progression. Luciferase-Gli261 cells were intracranially injected into RosaCre-ERT2/PDGFR $\alpha^{fl/fl}$ mice and RosaCre-ERT2/PDGFR $\alpha^{+/+}$ mice. **A**, tumor burden is represented by photon flux intensity. Means \pm SD, $n = 10$ mice; t test, *, $P < 0.05$. **B**, precontrast and postcontrast T1-weighted MRIs were performed on each group at day 15. Arrows, enhancing tumor. Tumor volume quantification is demonstrated. Means \pm SD, $n = 5$ mice; t test, **, $P < 0.01$. **C**, vWF was stained in the tumor periphery and within the tumor of each group (left and middle panels). Collagen IV was stained in each group (right). Scale bar, 50 μ m. Vessel diameters were quantified. Means \pm SD, $n = 6$ mice; t test, *, $P < 0.05$.

cells with GFP and allowed them to form tubules. Once a tubule network was established, equal numbers of GA-OPCs and astrocytes were introduced to the endothelial cell cultures. The *in vitro* 3D coculture system recapitulated the *in vivo* phenomenon within which the astrocytic foot processes surround endothelium to form the blood–brain barrier. We found that both astrocytes and GA-OPCs were adjacent to the endothelial tubules. Astrocytic foot processes formed an intact and continuous tubule-like structure close to endothelial tubules. In contrast, GA-OPCs appeared to integrate with the endothelial tubules but did not form continuous intercellular interaction with each other as did astrocytes (Fig. 4A). Interestingly, if we allowed astrocytes to establish interaction with HCMEC/D3 first with coculture, and then added GA-OPCs, the GA-OPCs could disrupt the interaction formed between astrocytes (Fig. 4A). We further used *in vitro* models to test the permeability of these intercellular interactions, which were formed by endothelial cells under differing coculture conditions. These assays demonstrated that astrocytes protect the integrity of the endothelial cell monolayer while bathed in U251 cell-derived conditioned medium, whereas GA-OPCs abrogate the protective effect of astrocytes by creating a more permeable endothelial cell monolayer (Supplementary Fig. S6C).

In addition to defining interactions between endothelial cells, astrocytes, and GA-OPCs, we performed a series of angiogenesis assays to study the mechanism through which GA-OPCs impact vascular remodeling. We used a sprouting assay to investigate the influence of perivascular stromal cells upon the migration of endothelial cells. Astrocytes suppressed

sprouting from endothelial spheres made from HCMEC/D3; GA-OPCs reversed this inhibitory effect when cocultured with astrocytes (Fig. 4B). We also analyzed the number of endothelial cells in coculture with astrocytes and GA-OPCs. Both astrocytes and GA-OPCs only minimally affected the number of endothelial cells (Supplementary Fig. S5D), suggesting that the regulatory effect of stromal cells on endothelial sprouting was proliferation independent. This function is PDGFR α dependent; a neutralizing PDGFR α -specific antibody reversed the effect (Supplementary Fig. S6A). Tubule formation assays similarly demonstrated that astrocytes inhibited the formation of new endothelial tubules and GA-OPCs reversed this in a PDGFR α signaling-dependent manner (Fig. 4C and Supplementary Fig. S6B).

How these interactions between endothelial cells and OPCs directly affect the tumor progression is difficult to precisely define. We have demonstrated that inhibiting OPCs clearly affects angiogenesis, which might then inhibit tumor progression. More interestingly, there may also exist a direct link between endothelial and tumor cells. We hypothesized that OPCs may direct endothelial cells into a more active state through upregulation of angiocrine factors, thereby promoting malignancy. We cocultured endothelial cells with Gli261 cells in the presence or absence of VEGF (to stimulate endothelial cells). We found that tumor cells proliferated more when cocultured with activated endothelial cells than when cocultured with normal endothelial cells (Supplementary Fig. S7). Considering the complex nature of the glioma microenvironment, interaction between OPCs and endothelial cells may be

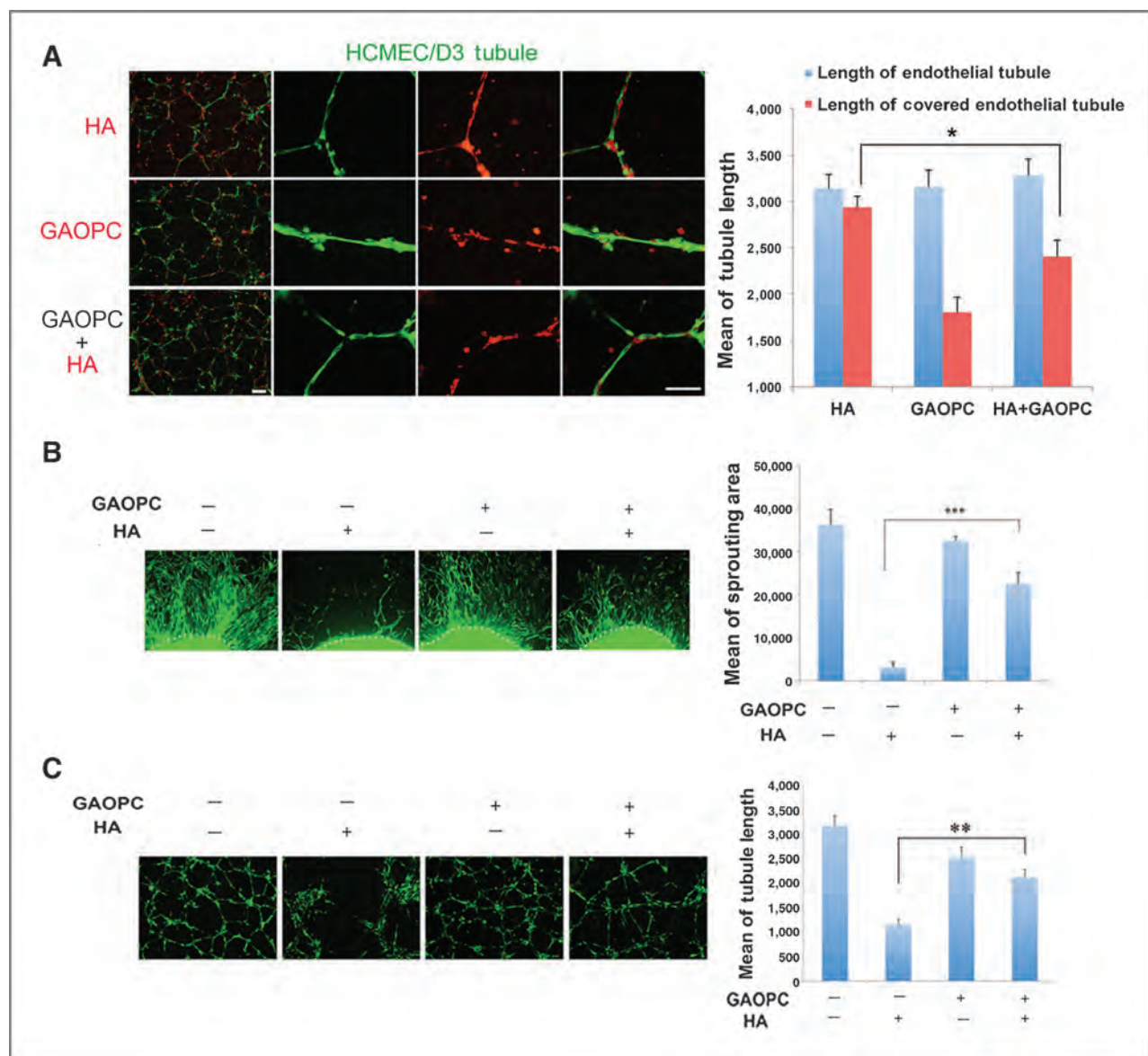


Figure 4. GA-OPCs promote opening of the endothelial-astrocytic junction and angiogenic activity of endothelial cells. **A**, GFP⁺ HCMEC/D3 cells (green) were seeded in Matrigel to assess tubule formation. Rodamine labeled (red), human astrocytes (HA), and GA-OPC were added subsequently. For the combination of human astrocytes and OPCs, labeled human astrocytes were allowed to seed with endothelial tubules first, followed by nonlabeled GA-OPCs 12 hours later. Scale bar of the first left panel, 100 μ m. Scale bar of right three panels, 50 μ m. GFP⁺ endothelial tubules' length and coverage were quantified. Means \pm SEM, $n = 5$; one-way ANOVA, *, $P < 0.05$. **B**, coculture with human astrocytes, GA-OPC (glioma associated OPCs), or both. The coculture system was maintained in U251-conditioned medium. Endothelial sprouting was quantified by the area of endothelial cells beyond the primary spheroid (dashed lines). Means \pm SEM, $n = 6$; one-way ANOVA, ***, $P < 0.001$. **C**, GFP-HCMEC/D3 cells were seeded on Matrigel to form tubules, cocultured with GA-OPC, human astrocytes, or both, and maintained in U251-conditioned medium. The GFP⁺ endothelial tubules in each group were quantified by length. Means \pm SEM, $n = 6$; one-way ANOVA, **, $P < 0.01$. All graphs were acquired from two independent experiments. N , the number of independent wells of treatment per condition.

even more complicated than that hypothesized with multiple pathways independently promoting malignancy.

BMDCs and stromal-derived PDGF-CC are key mediators to GA-OPCs

In the context of the glioma microenvironment, OPCs exponentially increase in number and in the expression of PDGFR α (Fig. 1). Signaling that originates from tumor-initiating or alternative stromal cells might trigger OPC

activation and redirect them into protumoral phenotypes. As described above, the number of PDGFR α ⁺ cells dramatically increased around day 14 after injection of tumor cells, which mirrored the pattern of immune cell infiltration (Fig. 1A and B). Therefore, we sought to test the hypothesis that infiltrating BMDCs contribute to the recruitment and activation of GA-OPCs during tumor progression. In addition, BMDCs are detected not only intratumorally, but also within the tumor periphery (Fig. 1A), a localization that would

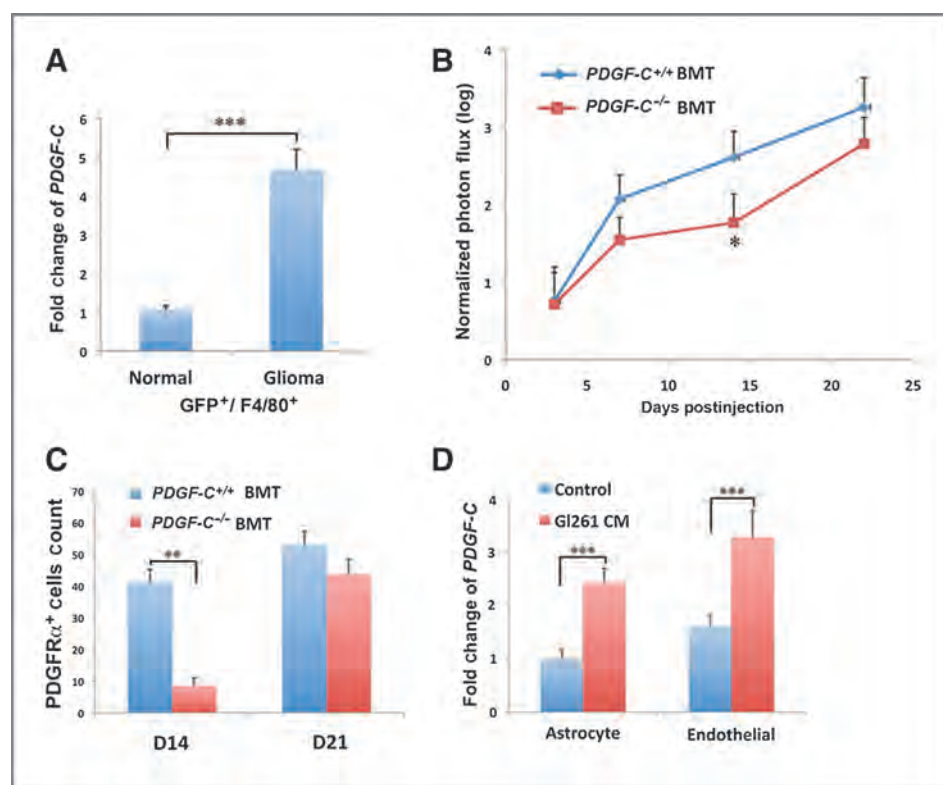


Figure 5. Stromal derived PDGF-CC serves as an activator of OPCs in glioma. **A**, PDGF-C is upregulated in glioma-associated macrophages. Quantitative RT-PCR of PDGF-C on GFP⁺/F4/80⁺ macrophage/microglia sorted from orthotopic Gli261 tumors or normal brain. Means \pm SEM, $n = 6$ mice; t test, ***, $P < 0.001$. **B**, the growth of Gli261 tumors in mice transplanted with PDGF-C^{-/-} bone marrow or littermate PDGF-C^{+/+} bone marrow was measured by photon flux. Means \pm SD, $n = 8$ mice; t test, *, $P < 0.05$. **C**, PDGFR α ⁺ cells were quantified in the tumor periphery of Gli261 tumors at D14 and D21, respectively, from both PDGF-C^{-/-} and PDGF-C^{+/+} BMT animals. Means \pm SEM, $n = 5$ mice; one-way ANOVA, **, $P < 0.01$. **D**, endothelial cells and astrocytes isolated from cortical tissue of C57BL/6 mice were treated with Gli261 conditioned medium or control medium. Quantitative RT-PCR of PDGF-C was performed, demonstrating the upregulation of PDGF-C in both endothelial and astrocytic cells in response to glioma conditions. Means \pm SEM, $n = 6$; t test, ***, $P < 0.001$. The graph was acquired from two independent experiments. N , the number of independent wells of treatment per condition.

permit direct BMDs/GA-OPCs interactions. Subsequently, we further characterized the infiltrating GFP⁺ BMDs in Gli261-implanted mice, and found that more than 80% of the BMDs in these tumors are F4/80⁺ macrophages/microglial cells (Supplementary Fig. S8A). We then performed microarray analysis on GFP⁺/F4/80⁺ BMDs, and found that the *PDGF-C* gene was significantly upregulated in glioma-associated BMDs compared with BMDs from normal murine brain (Supplementary Fig. S8B). *PDGF-C* is a cytokine that preferentially homodimerizes into PDGF-CC, which is the ligand predominantly binding PDGFR α . The upregulation of *PDGF-C* in bone marrow-derived macrophage/microglia isolated from murine gliomas was confirmed by real-time PCR (RT-PCR; Fig. 5A).

PDGF-C deletion recapitulates PDGFR α null phenotype

To examine whether PDGF-CC derived from bone marrow-derived macrophages or microglial cells might push GA-OPCs into tumor-supporting phenotypes, we transplanted wild type C57BL/6 mice with bone marrow from PDGF-C^{-/-} donor mice. Six weeks after bone marrow engraftment, luciferase-labeled Gli261 cells were injected intracranially into recipient mice. PDGF-C^{-/-} mice did not show any developmental defects in

their hematopoietic system (Supplementary Fig. S9); however, we found that tumors implanted within mice transplanted with PDGF-C^{-/-} bone marrow grew more slowly at an early stage of tumorigenesis (day 14) than tumors in mice transplanted with littermate PDGF-C^{+/+} bone marrow. However, in later stages (day 21) of tumor growth, PDGF-C^{-/-} bone marrow-transplanted animals no longer demonstrated a statistically significant reduction of tumor size (Fig. 5B). Within the tumor periphery specifically, we found significantly fewer PDGFR α ⁺ cells in the PDGF-C^{-/-} bone marrow-transplanted group at D14 ($P = 0.0051$), but not at a later stage (D21; $P = 0.32$; Fig. 5C). These results suggest that microphage-/microglia-derived PDGF-CC did contribute to the recruitment and activation of GA-OPCs, a process not necessarily dependent upon bone marrow-derived macrophages/microglia at later stages of tumor development.

Soluble PDGF-CC may not be solely secreted by BMDs; thus, we inferred that other stromal cells within the glioma microenvironment such as residential microglia, activated astrocytes, or angiogenic endothelial cells could be candidates as sources of soluble PDGF-CC. Therefore, we tested *PDGF-C* expression in astrocytes and endothelial cells in response to tumor cells. Primary cultures of astrocytes and endothelial

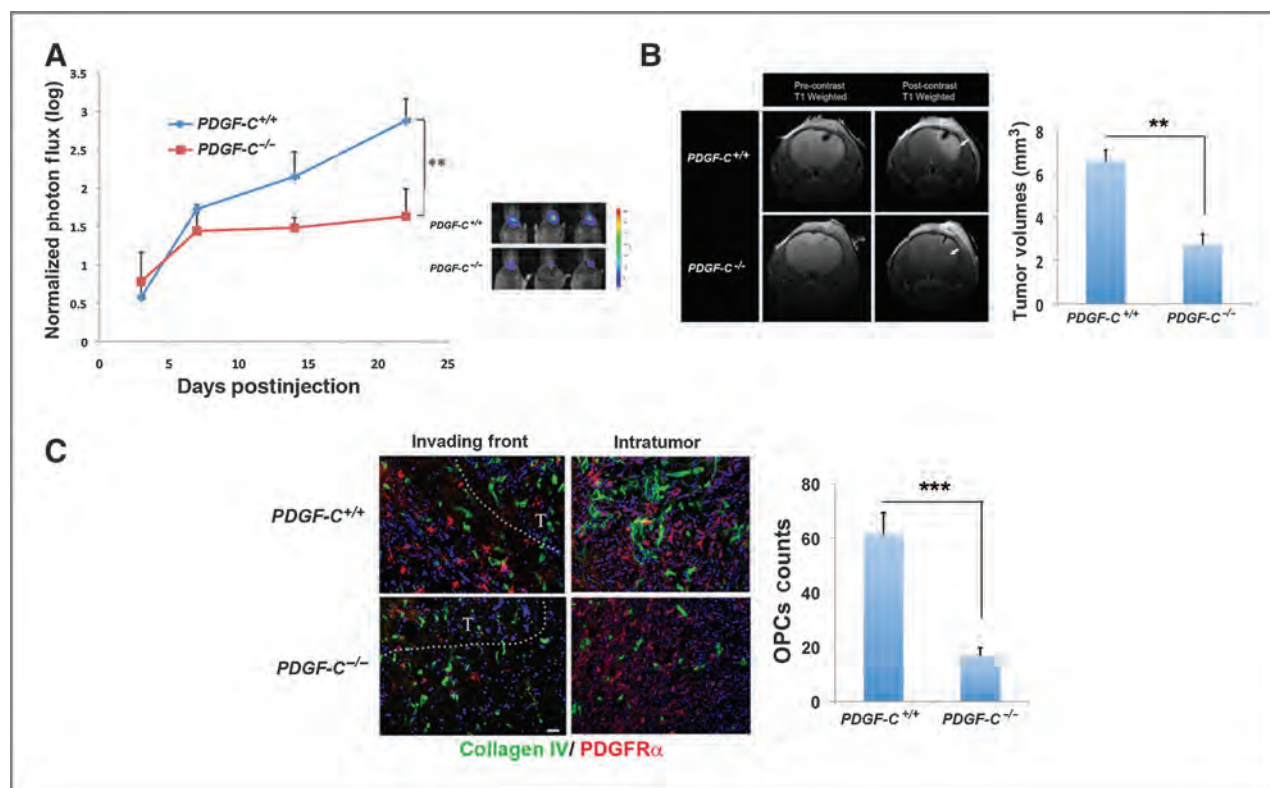


Figure 6. Glioma growth in PDGF-C deficient mice is phenotypically similar to glioma growth in PDGFR α KO mice. **A**, growth of orthotopic Gli261 tumors in PDGF-C^{-/-} and PDGF-C^{+/+} mice. Tumor burden is represented by bioluminescence photon flux. Means \pm SD, $n = 8$ mice; t test, **, $P < 0.01$. **B**, pre- and post-contrast T1-weighted MRI was used to image Gli261 tumors in PDGF-C^{-/-} animals and PDGF-C^{+/+} animals on day 17. Arrows, the enhancing tumor region. Tumor volumes were quantified. Means \pm SD, $n = 5$ mice; t test, **, $P < 0.01$. **C**, PDGFR α ⁺ cells were decreased in PDGF-C^{-/-} mice. Blood vessels (collagen IV) and PDGFR α were stained in both the invasive tumor front (invading front) and from within Gli261 tumors (intratumor) grown in the PDGF-C^{-/-} group and the PDGF-C^{+/+} group. Scale bar, 50 μ m. Means \pm SD, $n = 5$ mice; t test, ***, $P < 0.001$.

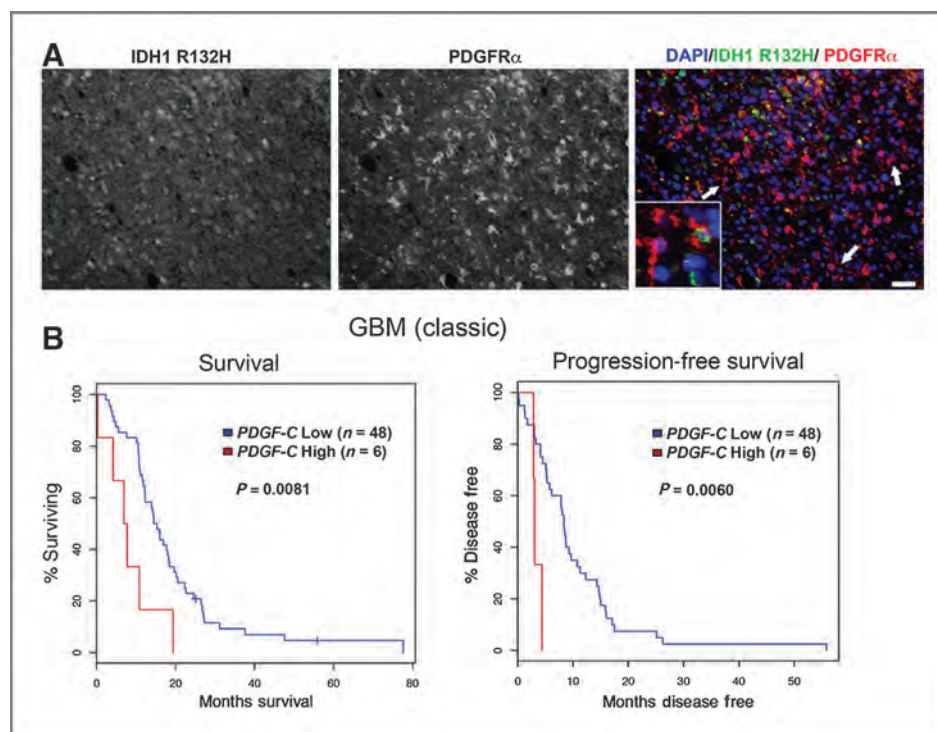
cells were isolated from mouse brain, and treated with or without conditioned medium derived from Gli261 cell culture. RT-PCR from both primary cultures showed that the expression of *PDGF-C* was upregulated by tumor-conditioned medium (Fig. 5D), implying that PDGF-CC might be expressed and secreted by glioma-associated astrocytes and endothelial cells. However, we found that other types of tumor cells, including B16/F10 and KR158, could both upregulate the *PDGF-C* expression within stromal cells (Supplementary Fig. S10A), suggesting that the upregulation of *PDGF-C* may be specific to glioma stroma, but not to tumor cells. The stromal-derived PDGF-CC may also be related to other cancers and proinflammatory states.

To assess the contribution of total stromal PDGF-CC to gliomagenesis, we intracranially injected Gli261 cells into PDGF-C^{-/-} knockout mice. Gli261 tumor growth in PDGF-C^{-/-} mice was significantly slower, and tumor burden was less than the tumors in littermate PDGF-C^{+/+} mice (Fig. 6A and B). MRI demonstrated strikingly less tumor enhancement in PDGF-C^{-/-} mice. These results recapitulated the phenotype of Gli261 tumor progression in PDGFR α knockout mice. More importantly, we found many fewer PDGFR α ⁺ cells in the tumor periphery in PDGF-C^{-/-} mice and significantly smaller vascular lumens (Fig. 6C). Taken together, these results demonstrate

that stromal-derived PDGF-CC is a key mediator in the recruitment and activation of OPCs during the progression of gliomas.

PDGF-CC, of which the primary receptor is PDGFR α , has been implicated in various cell types and pathologic conditions. A recent study showed that PDGF-CC knockout mice showed abnormal cerebral vascularization (28), supporting the role of PDGF-CC in regulating the vascular architecture under physiologic conditions in the CNS. In the postnatal brain, PDGFR α is exclusively expressed on OPCs (29). Thus, the stromal PDGF-CC/PDGFR α axis may be an important intrinsic angiogenic signaling pathway regulating angiogenesis in gliomas—independent of the classic VEGF-mediated pathway. To further understand the role of this signaling axis in regulating angiogenesis, we used an angiogenesis antibody array (R&D systems) to profile the angiogenic factors derived from OPCs after the exposure to PDGF-CC. PDGF-CC upregulated proangiogenic factors such as CXCL10, CX3CL1, and IGFBP-1 in OPCs (Supplementary Fig. S10B). PDGF-AA, PDGF-AB, PDGF-BB, and VEGF remained unchanged in the same assay. Among upregulated factors, OPC-derived MMP9 was recently found to mediate blood-brain barrier opening in response to white matter injury (26). These results indicate that GA-OPCs might have a direct impact upon activating endothelial cells and recruiting proangiogenic myeloid cells.

Figure 7. Human glioblastoma (GBM) samples from TCGA support a role for the PDGF-signaling axis. **A**, patient samples show GA-OPCs. Sections from IDH mutant-positive/grade III astrocytomas were stained with an antibody against IDH R132H and PDGFR α . Arrow demonstrates PDGFR α + IDH R132H cells. The inset shows an enlarged image. Scale bar, 50 μ m. **B**, PDGF-C levels are reversely correlated with glioblastoma patient's survival. The overall survival and progression-free survival of patients with glioblastoma were analyzed based on the expression of PDGF-C by using data from TCGA in the classic subtype of glioblastoma. Survival, $P = 0.008$; progression-free survival, $P = 0.006$ by the log-rank test.



GA-OPCs in patients with glioma

The brain tumor microenvironment in patients with glioma is very complex. The signaling within undefined stromal populations and tumor cells is intricate. This is further complicated by the molecular heterogeneity between subpopulations of actual glial tumor cells. Therefore, we sought to confirm and quantify the existence of PDGFR α + stromal cells directly from samples resected from patients diagnosed with a high-grade glioma. Among established markers for glioma cells, isocitrate dehydrogenase 1 (IDH1) mutation is extremely reliable in distinguishing tumor cells from stromal cells as it has been used to detect even single disseminated tumor cells (30, 31). Grade III astrocytomas bearing IDH1 mutations were chosen, and stromal cells were characterized as negative for the IDH mutation. Doubly staining for PDGFR α and IDH (R231H), we demonstrated a population of cells positive for PDGFR α and negative for IDH (R231H; Fig. 7A). Interestingly, this region was actively undergoing microvascular proliferation evidenced by enlarged vascular lumens (Supplementary Fig. S11).

As we demonstrated in our animal glioma models, PDGF-CC is a potential ligand through which the activation of GA-OPCs may occur, thereby contributing to angiogenesis and glioma progression. In *PDGF-C* null mice, glioma progression was slowed due to a lack of activated GA-OPCs. We examined the expression of *PDGF-C* in different types of gliomas within Rembrandt. We observed that expression levels of *PDGF-C* were higher in high-grade gliomas as compared with low-grade gliomas or nontumor diseases (Supplementary Fig. S12). To further study the role of PDGF-CC in human high-grade gliomas, data from The Cancer Genome Atlas (TCGA) for different

subsets of patients with glioblastoma were analyzed based on their expression of *PDGF-C*. Samples were subgrouped into those with higher *PDGF-C* expression (top 10–14%) with the remainder classified as *PDGF-C* low. Analyses of survival and progression were performed within four recognized subsets of glioblastoma, including classic, proneural, mesenchymal, and neural. Within the classic subset of glioblastoma, but not in other subsets, expression of *PDGF-C* was significantly correlated with disease progression ($P = 0.0060$), and inversely correlated with survival of patients ($P = 0.0081$; Fig. 7B and Supplementary Fig. S13). This demonstration within the classic subset of human glioblastoma is consistent with our demonstrated slowing of orthotopic G1261 tumor progression in *PDGF-C* null mice. Surprisingly, even other members of the PDGF family, including *PDGF-A* and *PDGF-B*, commonly upregulated in glioblastoma, were not found to be statistically significantly ($P > 0.05$) correlated with patients' survival or disease progression (Supplementary Fig. S14).

Discussion

OPCs are the most abundant neural progenitor cells in postnatal brains. They can differentiate into oligodendrocytes or astrocytes in response to different stimuli to aid in myelination and wound healing, among other roles in the CNS (32–36). Recent studies also suggest that OPCs have a higher degree of plasticity and may be more sensitive to transformation (9, 10). In certain rodent brain tumor models, it has been demonstrated that recruited stromal OPCs can be tumorigenic. However, their transformation of OPCs may require a preexisting oncogenic mutation such as *Ink4a/Arf* or *P53* as indicated by these studies (37).

Invasive glioma cells frequently migrate along myelinated white matter fiber tracts (38), a phenomenon whose underlying mechanism is not clearly elucidated. It has also been established that OPCs preferentially reside along identical pathways of dissemination (39, 40). Many studies have examined and demonstrated that glioma progression and invasion follows a perivascular pattern (25, 41, 42), particularly at disease recurrence. In this study, we demonstrated angiogenic endothelial cells, perivascular macrophages/microglia, and OPCs working in concert to form a proangiogenic and proinvasive niche at the invading front of glioma. Our data suggest that stromal OPCs are a key element not only in initiating angiogenesis but also in driving glioma invasion. To extend our hypotheses derived from mouse models to humans, we selected IDH1R132H mutant grade III astrocytomas within which to analyze stromal PDGFR α ⁺ cells from human specimens. The IDH1 R132H mutation is an ideal marker to distinguish between tumor cells and stromal cells in grade III astrocytomas. In addition, grade III astrocytomas are by definition in the transition stage, during which we suggest that OPCs play a crucial role in both microvascular proliferation and tumor invasion.

In the previous work, PDGF-CC was found to induce the loss of the blood–brain barrier and induce vascular leakiness in a stroke model, and PDGF-C deficiency leads to abnormal cerebral vascularization (28, 43). In our study in tumor-bearing mice, the number of OPCs with activated PDGFR α was increased compared with non-tumor-bearing mice. However, similar tumors could not increase the number of OPCs in PDGF-C^{−/−} mice. Interestingly, PDGF-CC has been identified as a key factor allowing tumors to recur following the anti-VEGF treatment in glioblastoma and other types of cancer (44, 45). All of this evidence suggests that PDGF-CC plays an important role in the vascular remodeling occurring in gliomas, which may be independent of the classic VEGF pathway. When studying survival using the glioblastoma cohort in TCGA, we demonstrated a survival advantage correlating with the *PDGF-C* expression only in the classic subgroup of glioblastoma. We hypothesize that the correlation within the classic subgroup might be due to differences of the origin of

tumor cells between the subgroups of glioblastoma. Mesenchymal, or proneural subtypes may be derived directly from OPCs where it has been suggested that tumor cells may inherit certain features directly from OPCs. In this class of glioblastoma, the tumor cells may overshadow stromal OPCs with respect to their proangiogenic role. Recent studies have demonstrated that tumor cells may transdifferentiate into endothelial cells and pericytes (46–48). This finding suggests that tumor heterogeneity along with the complex nature of the tumor microenvironment can result in the utilization of multiple angiogenic pathways.

Disclosure of Potential Conflicts of Interest

No potential conflicts of interest were disclosed.

Authors' Contributions

Conception and design: Y. Huang, D. Lyden, J.P. Greenfield

Development of methodology: Y. Huang, B. Weksler

Acquisition of data (provided animals, acquired and managed patients, provided facilities, etc.): Y. Huang, C. Hoffman, P. Rajappa, J.-H. Kim

Analysis and interpretation of data (e.g., statistical analysis, biostatistics, computational analysis): Y. Huang, P. Rajappa, J.-H. Kim, W. Hu, J. Bromberg, J.P. Greenfield

Writing, review, and/or revision of the manuscript: Y. Huang, C. Hoffman, P. Rajappa, J.-H. Kim, J.T. Huse, Z. Tang, X. Li, B. Weksler, J. Bromberg, D. Lyden, J.P. Greenfield

Administrative, technical, or material support (i.e., reporting or organizing data, constructing databases): J.T. Huse, Z. Tang, X. Li

Study supervision: D. Lyden, J.P. Greenfield

Acknowledgments

The authors thank Dr. Irina Matei for manuscript editing, Drs. Tyler Jacks and Karlyne Reilly for providing KR158 cells, Dr. David Zagzag for providing GL261 cells, Scott Kerns for imaging assistance, and Eric Aronowitz for MRI assistance.

Grant Support

This study was supported by DoD CDMRP (CA120318), Elizabeth's Hope, and The Matthew Larson Foundation.

The costs of publication of this article were defrayed in part by the payment of page charges. This article must therefore be hereby marked *advertisement* in accordance with 18 U.S.C. Section 1734 solely to indicate this fact.

Received April 15, 2013; revised December 2, 2013; accepted December 6, 2013; published OnlineFirst December 26, 2013.

References

- Charles NA, Holland EC, Gilbertson R, Glass R, Kettenmann H. The brain tumor microenvironment. *Glia* 2011;59:1169–80.
- Joyce JA, Pollard JW. Microenvironmental regulation of metastasis. *Nat Rev Cancer* 2009;9:239–52.
- Hanahan D, Weinberg RA. Hallmarks of cancer: the next generation. *Cell* 2011;144:646–74.
- Abbott NJ, Ronnback L, Hansson E. Astrocyte-endothelial interactions at the blood-brain barrier. *Nat Rev Neurosci* 2006;7:41–53.
- Barres BA, Raff MC. Axonal control of oligodendrocyte development. *J Cell Biol* 1999;147:1123–8.
- Shih AH, Dai CK, Hu XY, Rosenblum MK, Koutcher JA, Holland EC. Dose-dependent effects of platelet-derived growth factor-B on glial tumorigenesis. *Cancer Res* 2004;64:4783–9.
- Huse JT, Holland EC. Targeting brain cancer: advances in the molecular pathology of malignant glioma and medulloblastoma. *Nat Rev Cancer* 2010;10:319–31.
- Verhaak RG, Hoadley KA, Purdom E, Wang V, Qi Y, Wilkerson MD, et al. Integrated genomic analysis identifies clinically relevant subtypes of glioblastoma characterized by abnormalities in PDGFRA, IDH1, EGFR, and NF1. *Cancer Cell* 2010;17:98–110.
- Liu C, Sage JC, Miller MR, Verhaak RGW, Hippenmeyer S, Vogel H, et al. Mosaic analysis with double markers reveals tumor cell of origin in glioma. *Cell* 2011;146:209–21.
- Sugiarto S, Persson AI, Munoz EG, Waldhuber M, Lamagna C, Andor N, et al. Asymmetry-defective oligodendrocyte progenitors are glioma precursors. *Cancer Cell* 2011;20:328–40.
- Lindberg N, Kastemar M, Olofsson T, Smits A, Uhrbom L. Oligodendrocyte progenitor cells can act as cell of origin for experimental glioma. *Oncogene* 2009;28:2266–75.
- Persson AI, Petritsch C, Swartling FJ, Itsara M, Sim FJ, Auvergne R, et al. Non-stem cell origin for oligodendroglioma. *Cancer Cell* 2010;18:669–82.
- Dawson MR, Polito A, Levine JM, Reynolds R. NG2-expressing glial progenitor cells: an abundant and widespread population of cycling cells in the adult rat CNS. *Mol Cell Neurosci* 2003;24:476–88.

14. Geha S, Pallud J, Junier MP, Devaux B, Leonard N, Chassoux F, et al. NG2+/Olig2+ cells are the major cycle-related cell population of the adult human normal brain. *Brain Pathol* 2009;20:399–411.
15. Phillips HS, Kharbanda S, Chen RH, Forrest WF, Soriano RH, Wu TD, et al. Molecular subclasses of high-grade glioma predict prognosis, delineate a pattern of disease progression, and resemble stages in neurogenesis. *Cancer Cell* 2006;9:157–73.
16. Tang Z, Arjunan P, Lee C, Li Y, Kumar A, Hou X, et al. Survival effect of PDGF-CC rescues neurons from apoptosis in both brain and retina by regulating GSK3beta phosphorylation. *J Exp Med* 2010;207:867–80.
17. Newcomb EW, Tamasdan C, Entzminger Y, Arena E, Schnee T, Kim M, et al. Flavopiridol inhibits the growth of GL261 gliomas in vivo: implications for malignant glioma therapy. *Cell Cycle* 2004;3:230–4.
18. Reilly KM, Loisel DA, Bronson RT, McLaughlin ME, Jacks T. Nf1;Trp53 mutant mice develop glioblastoma with evidence of strain-specific effects. *Nat Genet* 2000;26:109–13.
19. Miyatake SI, Martuza RL, Rabkin SD. Defective herpes simplex virus vectors expressing thymidine kinase for the treatment of malignant glioma. *Cancer Gene Ther* 1997;4:222–8.
20. Weksler BB, Subileau EA, Perriere N, Charneau P, Holloway K, Leveque M, et al. Blood-brain barrier-specific properties of a human adult brain endothelial cell line. *FASEB J* 2005;19:1872–4.
21. Kawakami K, Kioi M, Liu Q, Kawakami M, Puri RK. Evidence that IL-13R alpha-2 chain in human glioma cells is responsible for the antitumor activity mediated by receptor-directed cytotoxin therapy. *J Immunother* 2005;28:193–202.
22. Kaplan RN, Riba RD, Zacharoulis S, Bramley AH, Vincent L, Costa C, et al. VEGFR1-positive haematopoietic bone marrow progenitors initiate the pre-metastatic niche. *Nature* 2005;438:820–7.
23. Huang YJ, Song N, Ding YP, Yuan SP, Li XH, Cai HC, et al. Pulmonary vascular destabilization in the premetastatic phase facilitates lung metastasis. *Cancer Res* 2009;69:7529–37.
24. Peinado H, Rafii S, Lyden D. Inflammation joins the "Niche". *Cancer Cell* 2008;14:347–9.
25. Calabrese C, Poppleton H, Kocak M, Hogg TL, Fuller C, Hamner B, et al. A perivascular niche for brain tumor stem cells. *Cancer Cell* 2007;11:69–82.
26. Seo JH, Miyamoto N, Hayakawa K, Pham LD, Maki T, Ayata C, et al. Oligodendrocyte precursors induce early blood-brain barrier opening after white matter injury. *J Clin Invest* 2013;123:782–6.
27. Louis DN, Ohgaki H, Wiestler OD, Cavenee WK, Burger PC, Jouvet A, et al. The 2007 WHO classification of tumours of the central nervous system. *Acta Neuropathol* 2007;114:97–109.
28. Fredriksson L, Nilsson I, Su EJ, Andrae J, Ding H, Betsholtz C, et al. Platelet-derived growth factor C deficiency in C57BL/6 mice leads to abnormal cerebral vascularization, loss of neuroependymal integrity, and ventricular abnormalities. *Am J Pathol* 2012;180:1136–44.
29. Sim FJ, McClain CR, Schanz SJ, Protack TL, Windrem MS, Goldman SA. CD140a identifies a population of highly myelinating, migration-competent and efficiently engrafting human oligodendrocyte progenitor cells. *Nat Biotechnol* 2011;29:934–U123.
30. Camelo-Piragua S, Jansen M, Ganguly A, Kim JC, Louis DN, Nutt CL. Mutant IDH1-specific immunohistochemistry distinguishes diffuse astrocytoma from astrocytosis. *Acta Neuropathol* 2010;119:509–11.
31. Capper D, Sahm F, Hartmann C, Meyermann R, von Deimling A, Schittenhelm J. Application of mutant IDH1 antibody to differentiate diffuse glioma from nonneoplastic central nervous system lesions and therapy-induced changes. *Am J Surg Pathol* 2010;34:1199–204.
32. Morello N, Bianchi FT, Marmiroli P, Tonoli E, Menendez VR, Silengo L, et al. A role for hemopexin in oligodendrocyte differentiation and myelin formation. *PLoS ONE* 2011;6:e20173.
33. Ziv Y, Avidan H, Pluchino S, Martino G, Schwartz M. Synergy between immune cells and adult neural stem/progenitor cells promotes functional recovery from spinal cord injury. *Proc Natl Acad Sci U S A* 2006;103:13174–9.
34. Lecca D, Trincavelli ML, Gelosa P, Sironi L, Ciana P, Fumagalli M, et al. The recently identified P2Y-like receptor GPR17 is a sensor of brain damage and a new target for brain repair. *PLoS ONE* 2008;3:e3579.
35. Chang A, Nishiyama A, Peterson J, Prineas J, Trapp BD. NG2-positive oligodendrocyte progenitor cells in adult human brain and multiple sclerosis lesions. *J Neurosci* 2000;20:6404–12.
36. Zawadzka M, Rivers LE, Fancy SPJ, Zhao C, Tripathi R, Jamen F, et al. CNS-resident glial progenitor/stem cells produce Schwann cells as well as oligodendrocytes during repair of CNS demyelination. *Cell Stem Cell* 2010;6:578–90.
37. Fomchenko EI, Dougherty JD, Helmy KY, Katz AM, Pietras A, Brennan C, et al. Recruited cells can become transformed and overtake PDGF-induced murine gliomas in vivo during tumor progression. *PLoS ONE* 2011;6:e20605.
38. Giese A, Bjerkvig R, Berens ME, Westphal M. Cost of migration: Invasion of malignant gliomas and implications for treatment. *J Clin Oncol* 2003;21:1624–36.
39. Grinspan JB, Stern JL, Pustilnik SM, Pleasure D. Cerebral white matter contains Pdgf-responsive precursors to O2a cells. *J Neurosci* 1990;10:1866–73.
40. Orentas DM, Miller RH. Regulation of oligodendrocyte development. *Mol Neurobiol* 1998;18:247–59.
41. Blouw B, Song HQ, Tihan T, Bosze J, Ferrara N, Gerber HP, et al. The hypoxic response of tumors is dependent on their microenvironment. *Cancer Cell* 2003;4:133–46.
42. Charles N, Ozawa T, Squatrito M, Bleau AM, Brennan CW, Hambardzumyan D, et al. Perivascular nitric oxide activates notch signaling and promotes stem-like character in PDGF-induced glioma cells. *Cell Stem Cell* 2010;6:141–52.
43. Su EJ, Fredriksson L, Geyer M, Folestad E, Cale J, Andrae J, et al. Activation of PDGF-CC by tissue plasminogen activator impairs blood-brain barrier integrity during ischemic stroke. *Nat Med* 2008;14:731–7.
44. Crawford Y, Kasman I, Yu LL, Zhong CL, Wu XM, Modrusan Z, et al. PDGF-C mediates the angiogenic and tumorigenic properties of fibroblasts associated with tumors refractory to anti-VEGF treatment. *Cancer Cell* 2009;15:21–34.
45. di Tomaso E, Snuderl M, Kamoun WS, Duda DG, Auluck PK, Fazlollahi L, et al. Glioblastoma recurrence after cediranib therapy in patients: lack of "rebound" revascularization as mode of escape. *Cancer Res* 2011;71:19–28.
46. Ricci-Vitiani L, Pallini R, Biffoni M, Todaro M, Invernici G, Cenci T, et al. Tumour vascularization via endothelial differentiation of glioblastoma stem-like cells. *Nature* 2010;468:824–8; corrigendum 2011;477:238.
47. Wang R, Chadalavada K, Wilshire J, Kowalik U, Hovinga KE, Geber A, et al. Glioblastoma stem-like cells give rise to tumour endothelium. *Nature* 2010;468:829–U128.
48. Cheng L, Huang Z, Zhou WC, Wu QL, Donnola S, Liu JK, et al. Glioblastoma stem cells generate vascular pericytes to support vessel function and tumor growth. *Cell* 2013;153:139–52.